Experimental drying shrinkage behaviour of concrete masonry for climate change design adaptation

By

Tonushri Das

June 9, 2023

Department of Civil Engineering and Applied Mechanics

McGill University, Montreal

A thesis submitted to the Faculty of Graduate Studies and Research in partial fulfillment of the requirements of the degree of Master of Engineering

Abstract

The analysis of the Climate Change Adaptation Standards inventory conducted by the Canadian Standards Association (CSA) in 2018 revealed the need for urgent provisions for climate change adaptation in cavity-wall design. The distress in masonry cavity-walls is often attributed to the differential movements between the outer veneer and inner loadbearing members. In the case of concrete masonry blocks used for structural backups, drying shrinkage phenomena are the primary cause of deformations leading to damage, which can worsen with the effects of climate change. However, the design of cavity-walls in Canada currently relies on outdated data that only pertains to individual concrete blocks. As part of a larger climate change design adaptation research project, this thesis paper presents a new testing methodology for unconstrained mortared concrete masonry prisms to gather insights on moisture-induced shrinkage and explore the influence of mechanical interaction between blocks and mortar. The methodology involves a two-step process where specimens are first allowed to dry from a saturated surface dry state over 12 weeks and then tested using the rapid method outlined in ASTM C426-06. The preliminary results and ongoing new results obtained are in good agreement with those obtained by previous Canadian researchers and suggest that the presence of mortar joints does not noticeably influence the shrinkage behaviour of the mortared concrete masonry assemblies tested so far. This research builds and tests an experimental infrastructure and framework that was not available at McGill University before, providing a significant contribution to the field. It aims to provide missing data to calibrate numerical models for designing cavity-walls in the future.

Resume

L'analyse de l'inventaire des normes d'adaptation aux changements climatiques menée par le Groupe CSA en 2018 a révélé le besoin urgent d'adaptation aux changements climatiques dans la conception des murs creux. La détérioration des murs creux en maçonnerie est souvent attribuée aux différents mouvements entre le placage extérieur et les éléments porteurs intérieurs. Dans le cas des blocs de maçonnerie en béton utilisés pour les appuis structuraux, les phénomènes de retrait dû au séchage sont la première cause de déformations entraînant des dommages, qui peuvent s'aggraver avec les effets du changement climatique. Cependant, la conception des murs creux au Canada repose actuellement sur des données désuètes qui ne concernent que des blocs de béton individuels. Dans le cadre d'un projet de recherche plus vaste d'adaptation de la conception au changement climatique, cette thèse présente une nouvelle méthodologie d'essai pour les prismes de maçonnerie en béton mortier sans contrainte afin de recueillir des informations sur le retrait induit par l'humidité et d'explorer l'influence de l'interaction mécanique entre les blocs et le mortier. La méthodologie implique un processus en deux étapes où les spécimens sont d'abord laissés sécher à partir d'un état surface saturé sêche pendant 12 semaines, puis testés à l'aide de la méthode rapide décrite dans la norme ASTM C426-06. Les résultats préliminaires et les résultats finaux en cours obtenus sont en bon accord avec ceux obtenus par les chercheurs canadiens antérieurs et suggèrent que la présence de joints de mortier n'influence pas sensiblement le comportement de retrait des assemblages de maçonnerie en béton mortier testés jusqu'à présent. Cette recherche construit et teste une infrastructure et un cadre expérimentaux qui n'étaient pas disponibles à l'Université McGill auparavant, apportant une contribution significative au domaine. Elle vise à fournir les données manquantes pour calibrer les modèles numériques pour la conception de murs creux à l'avenir.

Acknowledgements

Throughout the research process, I received invaluable guidance and supervision from Prof. Daniele Malomo, for which I am deeply grateful. In addition, I would like to express my appreciation to Adrien Sparling, my research group members and the laboratory technicians who provided valuable assistance in conducting the experiments. Their contributions were critical to the success of this research.

I would also like to extend my sincere gratitude to BLOCS MBM and O. Gravel for their generous donation of construction materials and to several organizations, including the Natural Sciences and Engineering Research Council of Canada (NSERC) through funding reference number ALLRP 573453-22, the Mitacs Accelerate program, the Canadian Masonry Design Centre (CMDC), and the Canadian Concrete Masonry Producers Association (CCMPA), for their support. Furthermore, I am immensely grateful for the Canadian Standard Association (CSA) scholarship program, which has significantly contributed to my studies.

Finally, I would like to acknowledge and thank the Canadian Society for Civil Engineering (CSCE) 2023 Annual Conference and the 14th North American Masonry Conference (14NAMC) for accepting and recognizing my research by presenting it at the conference and publishing it in the proceedings.

Contents

List of Figures

List of Tables

Thesis Organisation

This thesis paper, structured into five subsequent chapters, aims to discuss an innovative research project that investigates the experimental drying shrinkage behaviour of concrete masonry for climate change design adaptation. An experimental infrastructure and framework were devised from scratch and rigorously tested, both of which were previously unavailable at McGill University. The findings of this research have significant implications for climate-resilient design adaptation in the Canadian masonry construction industry and can contribute to the broader discourse on this topic. Additionally, this research will not only provide insights into concrete masonry's drying shrinkage behaviour but also lay the groundwork for future investigations. Below is a brief overview of the content of each chapter:

Chapter 1 introduces the key issues that frame the content of the thesis, namely concepts related to climate change risks and impacts on the Canadian masonry construction industry. The chapter also provides an extensive literature review on the subject matter, highlighting relevant research and practices on climate-resilient design adaptation.

Chapter 2 focuses on the experimental work of the research. It provides a detailed description of the methodology and infrastructure employed in the research. The chapter elaborates on the novel 2-step drying shrinkage experimental procedure that is central to the research work.

Chapter 3 discusses the preliminary and ongoing new results of the research. It analyzes the trends of shrinkage strain of each tested specimen and compares them with previous findings that use similar methods.

Chapter 4 concludes the paper by providing a summary of the key insights from the thesis. It highlights the implications of the research findings for the Canadian masonry construction industry and the broader discourse on climate-resilient design adaptation. The chapter also identifies potential areas for further research.

1 INTRODUCTION

1.1 Impact of climate change on Canada's masonry construction industry

Recent climate data analysis and modelling have shown that Canada's climate is changing at an alarming pace (Environment and Climate Change Canada, 2022). Since 1948, according to historical data of annual mean surface temperature, illustrated in **Error! Reference source not found.**, the annual average temperature over land has increased by approximately 1.7°C in Canada – roughly double the global average level of warming (Bush & Lemmen, 2019). The Canadian Arctic is warming even faster, at a rate equivalent to three times that of the globe as shown by the data gathered by the adjusted and homogenized Canadian climate data and the HadCRUT data in the graph below (Vincent, et al., 2015; Morice, Kennedy, Rayner, & Jones, 2012).

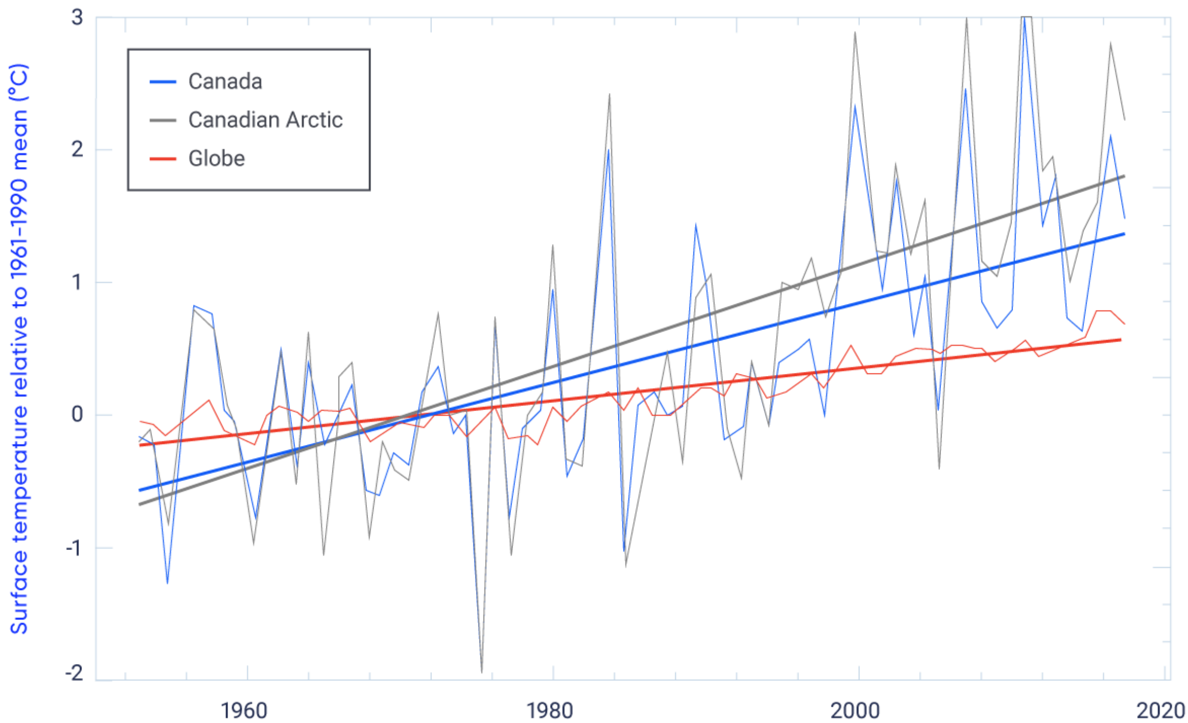

Figure 1: Rates of warming for Canada, the Canadian Arctic, and the world

The Canadian climate patterns are predicted to continue to significantly change in the imminent future as a result of the global phenomenon of anthropogenic climate change (Warren, et al., 2004). Considering both low and very high GHG emission scenarios, international model results predict the average temperatures in Canada to increase by 1.5°C to 4.5°C by 2070 (Cannon, Jeong, Zhang, & Zwiers, 2020).

While temperature changes have received the most attention in studies of global climate change, precipitation measurements also reveal long-term trends. With the increase in local temperature, more precipitation events are expected due to the increased moisture capacity of warm air. Canada has generally gotten wetter in recent decades, with an increase in yearly precipitation of roughly 16% between 1950 and 2009 (Mekis & Vincent, 2011). Figure 2 illustrates how this increase has varied across the country (Cannon, Jeong, Zhang, & Zwiers, 2020). The data suggest that southern Canada is likely to experience a shift from snow to rain as temperatures rise.

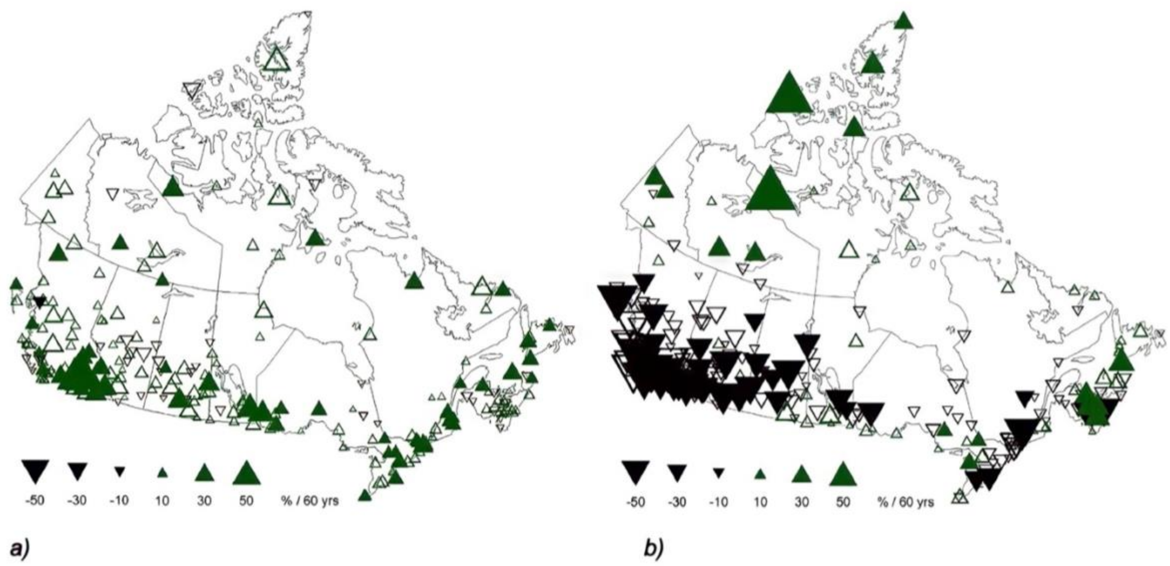

Figure 2: Observed annual precipitation trends 1950-2009
a) Rainfall b) Snowfall

Many sectors of the Canadian economy, including infrastructure, are experiencing the impacts of climate change both in the short and long term (Pravin, Murali, & Shanmugapriyan, 2017).

Built infrastructure, in particular, is identified as the most susceptible sector to climate change hazards, with direct costs projected to rise by over $40 billion per year by 2050 (The Council of Canadian Academies, 2019; National Round Table on the Environment and the Economy, 2011). Changes in temperature, precipitation, CO2 levels, and freeze-thaw cycles are causing early deterioration of building components, as well as increased exposure to natural disasters like earthquakes and tornadoes (Cannon, Jeong, Zhang, & Zwiers, 2020). Recognizing the importance of addressing the impacts of climate change on the built environment, Canada has made it a top priority and invested heavily in initiatives such as the *Pan-Canadian Framework on Clean Growth Plan* (> $100 billion, 2016-2027), *Canada Infrastructure Bank's Growth Plan* ($10 billion, 2020-2023), and the *Climate-Resilient Buildings and Core Public Infrastructure Initiative* (> $40 million, 2016-2027) (Environment and Climate Change Canada, 2016; Canada Infrastructure Bank, 2020; Cannon, Jeong, Zhang, & Zwiers, 2020). However, until recently, there has been a lack of research on the impacts of climate change on building design and durability. To address this, the National Research Council Canada (NRC) has established a comprehensive series of research programs to update building codes and design standards, which are crucial for ensuring the construction of more sustainable and less environmentally impactful structures and infrastructures (Government of Canada, 2022). Taking decisive actions to combat climate change is necessary to mitigate climate risks to physical infrastructure. According to projections from the National Round Table on Environment and the Economy (NRTEE) from 2011, the cost of inaction is expected to be higher than the cost of action, with climate change potentially costing Canada $21 to $43 billion annually by 2050 (National Round Table on the Environment and the Economy, 2011; Environment and Climate Change Canada, 2016).

While much attention is given to the direct impacts of climate change on people, wildlife, and ecosystems, it is important to recognize that buildings and infrastructure are also vulnerable to climate-related risks (Bush & Lemmen, 2019). Research groups in Canada (Lacasse, Gaur, & Moore, 2020; Zhou, Carmeliet, & Derome, 2020; Talukdar & Banthia, 2013) and abroad (Cavalagli, Kita, Castaldo, Pisello, & Ubertini, 2019; Saha & Eckelman, 2014; Hall, Hamilton, Hoff, Viles, & Eklund, 2010) has examined the ways in which climate change can exacerbate the degradation of building materials (Lacasse, Gaur, & Moore, 2020). This research has spurred a national effort in Canada to study the impacts of changing environmental conditions on building performance and durability (Gaur, Lacasse, & Armstrong, 2019). One recent initiative that highlights the need for climate-informed design adaptation strategies is the Climate Change Adaptation Standards Inventory Analysis conducted by the Canadian Standards Association (CSA) Group in 2018 (Sparling, Palermo, & Khan, 2021). This analysis examined the extent to which climate change could impact all 81 CSA standards listed in the 2015 National Model Codes, which provide guidance for design and construction in Canada. The masonry standard CSA A370-14 (*connectors for masonry*) was ranked in the top ten standards with "high priority" adaptation requirements, and several other masonry standards were also identified as having "medium priority" for climate change adaptation, including CSA A165.1-14/CSA A165.2-14 (*concrete block masonry units*) and CSA S304-14 (*design of masonry structures*) (Sparling, Palermo, & Khan, 2021). The adequacy of the best practices reported in these standards is projected to be directly and increasingly impacted by the changing climate. As such, new climate change-informed design adaptation strategies are required to ensure that masonry remains a durable option in the future.

Masonry is a popular construction material in Canada due to its numerous advantages, including heat and fire resistance, thermal mass and regulation properties, strength, and durability, making it a fundamental primary structural element or a long-lasting option for commercial, institutional, and residential buildings (Kubba, 2017). The Canadian masonry industry is a significant contributor to the economy, accounting for approximately 8% of the construction, renovation, and deconstruction work (Straka, 2005). Cavity-wall structures (see section 1.2), the most common type of masonry construction in Canada, are of particular concern due to their vulnerability to climate change impacts (Baker, Marr, & Drysdale, 2004). The Canadian Standards Association (CSA) recognizes the need for urgent climate change adaptation provisions in cavity-wall design (Sparling, Palermo, & Khan, 2021). Variations in freeze-thaw cycles (e.g., the annual number of cycles experienced by a structure or component) as well as changes in the corrosion environment of connectors due to changing precipitation and humidity patterns, are of particular significance to cavity-wall masonry assemblies (Aarle, Schellen, & Schijndel, 2015). Higher rates of carbonation in concrete have been linked to rising CO_2 levels in the atmosphere, which can accelerate the beginning of corrosion in cavity-walls (Yoon, Çopuroğlu, & Park, 2007). Therefore, understanding the mechanical and environmental behaviour of cavity-wall masonry structures is the first crucial step in predicting the necessary changes that must be incorporated into design standards to mitigate the impacts of climate change on the built environment.

1.2 Design adaptation of cavity-wall masonry construction

Among the different types of masonry wall construction, cavity-walls have been a common choice for Canadian builders in the last century. The term “cavity-wall” refers to a masonry structure with a double wall separated by an air gap with/without insulation/ventilation and coupled by metal connectors or ties (Ritchie, 1961). The inner wall constitutes the loadbearing masonry backup (typically concrete blocks) and the outer veneer (typically clay bricks) transmits external loads to the supporting structure also acting as a weather-resistant barrier. Metal connectors, or “ties” (see Figure 3), are anchored to the walls to provide the mechanical coupling between the two masonry leaves (Ritchie, 1961).

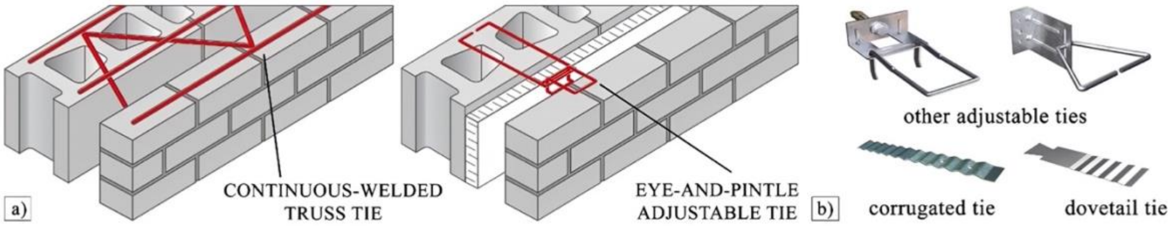

Figure 3: Typical construction details of masonry cavity-wall
a) Cross-section showing tie placement b) Shapes of ties

Other cavity-wall masonry key components include e.g., shelf-angles, movement joints, and insulation boards. A typical cavity-wall construction in Canada consists of an outer weather-resistant veneer that is 90 mm thick, an air space of 25 mm, insulation of 25 to 75 mm or more, and an interior backup wall that is 140 mm or thicker (Goyal, Hatzinikolas, & Warwaruk, 1992). Figure 4 shows a typical arrangement of a cavity wall, highlighting its most important structural components (Ismaiel, Chen, Cruz-Noguez, & Hagel, 2021).

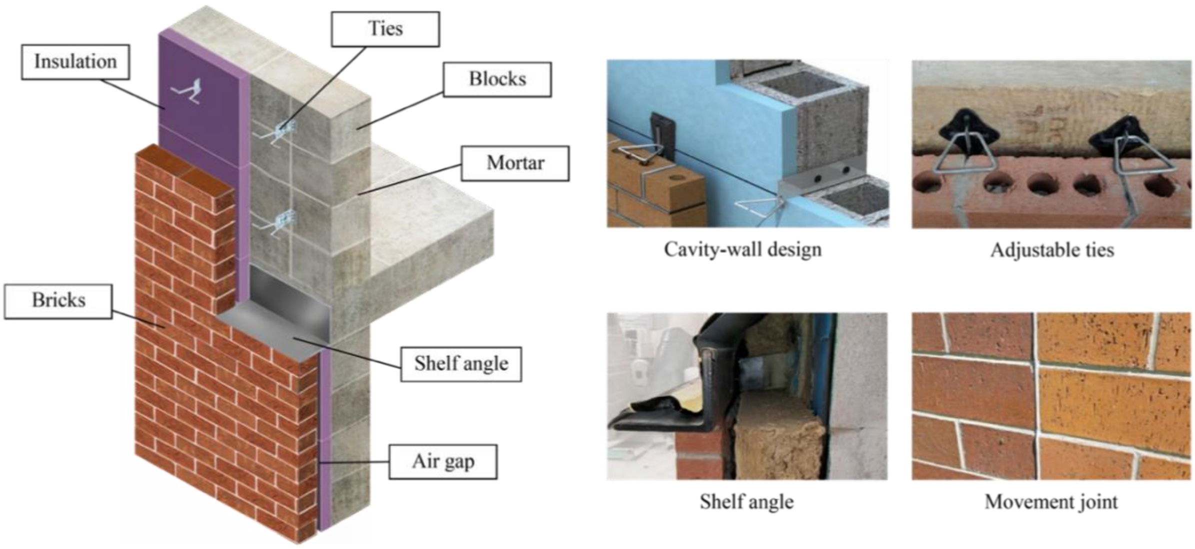

Figure 4: Typical construction details of masonry cavity-wall

Cavity-walls offer many advantages, including rapid construction, lower material requirements, and protection against rain penetration. The most significant advantage, however, is the improved thermal insulation that cavity-walls provide (Ritchie, 1961). Nevertheless, in addition to the need to reduce carbon emissions and comply with energy codes, climate change will soon require higher thermal efficiency at the building system level.

Improving the thermal energy efficiency of cavity-walls is an evolving step toward mitigating the extent of climate change impact on the built infrastructure (Ismaiel, Chen, Cruz-Noguez, & Hagel, 2021). Due to varying moisture content, the clay brick veneers in cavity-walls tend to expand while the concrete backup wythe may shrink, leading to early failures and localized fractures. While the temperature of the brick veneer tends to vary as it is exposed to the outer environment, the temperature of the backup wythe remains nearly constant. These temperature differences may create differential movement between the two wythes, generating unwanted concentrations of tension stresses inside the assembly (Goyal, Hatzinikolas, & Warwaruk, 1992). The impact of climate change will exacerbate these issues by increasing temperature and moisture-induced volumetric variations, resulting in cracks in the outer clay brick veneer and compromising durability. An effective and low-carbon emission measure to augment the thermal insulation of cavity-walls and reduce the impact of the abovementioned phenomena is the use of wider cavities beyond the values presently prescribed by CSA A370. As several design challenges and implications are related to this aspect, mechanical/environmental tests and numerical modelling are required to substantiate changes to the cavity-wall design guidelines of the following Canadian masonry standards: CSA A370-14 (*connectors for masonry*), CSA A165.1-14 (*concrete block masonry units*), and CSA S304-14 (*design of masonry structures*) (Canadian Standards Association, 2014). Adapting cavity-wall masonry structures to climate resilience requires reliable information on the properties of concrete masonry. Currently, available data on shrinkage behaviour pertains only to unit blocks, and it is unknown how the presence of mortar in masonry blocks affects assembly shrinkage in relation to unit blocks. This available data could therefore be obsolete. Given the present data are from decades ago, updated data on the shrinkage of concrete masonry, a leading cause of cracking and reduced durability, is essential for informed design and adaptation to a changing climate (Drysdale & Khattab, 1995).

1.3 Properties and performance of concrete masonry

The Canadian Standards Association (CSA) has identified four critical physical properties of these units that are important for element design and building performance in their CSA A165 standard. These include solid content, specified compressive strength, concrete type (density and absorption), and moisture content (Sturgeon, 2012). In addition to these physical properties, in terms of element design and building performance, the constructed concrete masonry units' considerations include fire resistance, sound control, and resistance to environmental loads (Sturgeon, 2012). As the resistance to compression is significantly higher than the resistance to tensile stresses, compressive strength is one of the most critical structural properties for modern masonry design and safety (Corradi, Tedeschi, Binda, & Borri, 2008). Compressive strength is a good indicator of the load-bearing capacity and the fired bond strength of concrete masonry (Sturgeon, 2012). According to the Canadian Masonry Structural Design Standard (CSA S304.1), several factors are considered to determine the specified compressive strength of concrete masonry, such as shear strength, modulus of elasticity, stiffness, serviceability, and bar reinforcement embedment (Sturgeon, 2012). The specified compressive strength is a direct function of the compressive strength of the masonry unit, the type of mortar used, and whether the unit is hollow or not. A large database of literature on masonry strength is available with different studies presenting various experimental values. Table 1 presents the most common range values of compressive and tensile strength for different masonry units and mortar (Canadian Standards Association, 2004).

Table 1: Specified compressive strength f'_m of concrete block masonry

Specified compressive strength of unit (average net area)	Type S mortar		Type N mortar	
	Hollow	Solid or Grouted	Hollow	Solid or Grouted
40 or more	22.0	17.0	14.0	10.5
30	17.5	13.5	12.0	9.0
20	13.0	10.0	10.0	7.5
15	9.8	7.5	8.0	6.0
10	6.5	5.0	6.0	4.5

In addition to the physical and structural properties of concrete block masonry units, concrete block masonry units are also classified based on their moisture content. Changes in the moisture content or relative humidity of the surrounding air can cause concrete to either lose or absorb moisture, leading to dimensional changes that can affect the overall stability and functionality of the structure. Before reaching an air-dry equilibrium condition, the cement paste may gain or lose moisture, causing it to "swell" or "shrink" respectively. When the moisture content of the concrete is in balance with the relative humidity of the surrounding environment, it will not alter its dimension (Sturgeon, 2012). Moisture content has a direct link to linear shrinkage characteristics as shown in Table 2 (Canadian Standards Association, 2004). To classify concrete block masonry units' linear shrinkage, CSA standards group them into three categories, expressed as a percentage of their initial (moisture-saturated) length. This classification is somewhat arbitrary and does not imply shrinkage limitations or suggest that units with lower characteristic shrinkage are superior. For each shrinkage classification, a moisture content limit is set as a percentage of the unit's 24-hour absorption. The limits listed in the table below depend on the relative humidity (RH) of the intended service environment (Sturgeon, 2012).

Table 2: Maximum moisture contents for concrete block masonry units

	Maximum Moisture Content (% of Total Absorption)	
Linear Shrinkage, %	Relative humidity over 75%	Relative humidity under 75%
< 0.03	45	40
0.003 to 0.045	40	35
> 0.045	35	30

1.4 Drying shrinkage of concrete masonry units

Changes in temperature and moisture cause most building materials to expand and/or contract. In addition to these changes in volume, movement is also caused by e.g., elastic deformations due to loads and/or creep. The restraint of these motions may result in tensile stresses inside building components, which can lead to cracks. Cavity-wall masonry elements should be constructed to limit these deformations and allow differential movement between materials and assemblies (Brick Industry Association, 2006; Goyal, Hatzinikolas, & Warwaruk, 1992). Concrete masonry units, particularly, is a construction material that experiences thermal, reversible moisture, elastic deformation, and creep movements (The American Institute of Architects, 2017). These units are composed of an aggregate particle matrix coated with cement that binds them together. This cementitious-coated aggregate matrix expands with rising moisture content and contracts with decreasing moisture content once the concrete has set. Moisture-induced movements usually result in net shrinkage of concrete masonry, which is influenced by the concrete characteristics and the ambient conditions. The major influencing factors include the technique and duration of curing, circumstance of storing, aggregate characteristics and dosage, water-cement ratio, cement type, air temperature, relative humidity, and wetting and drying cycles (Jianxia, 2012). Therefore, drying shrinkage is an effective test to evaluate the moisture movement in cavity-wall load-bearing backups. The total potential linear drying shrinkage owing to variations in moisture content is calculated using the standards edited by the American Society for Testing and Materials (ASTM), as the ASTM C426-06 *Test Method for Linear Drying Shrinkage of Concrete Masonry Units*, which measures unit shrinkage from a saturated to an equilibrium state at a relative humidity of 17% (American Society for Testing and Materials, 2006). For concrete masonry units, typical linear shrinkage values vary from $2 \cdot 10^{-4}$ to $4.5 \cdot 10^{-4}$ in./in. (mm/mm), and the coefficient of shrinkage is considered to equal half of the total linear shrinkage in the ASTM C426.-06 The drying shrinkage for an individual unit is controlled by the unit's wetness at the time of installation, as well as the properties and amount of cementitious materials, the aggregate type, consolidation, and curing (Saxer & Toennies, 1957). Shrinkage caused by drying in cavity-walls is influenced by multiple factors, including the following:

- cavity-walls made of wet units are more susceptible to greater drying shrinkage in comparison to walls made with dry units.
- drying shrinkage increases as cement content rises.
- shrinkage is greater in aggregates that are prone to volume change due to moisture content.
- units that have been through at least one drying cycle will shrink less in subsequent drying cycles (Saxer & Toennies, 1957).

To measure the shrinkage strains of concrete specimens, the placement of the points of measurement is an important factor, as depicted in Figure 5a, as it influences the determination of the coupled hygromechanical behaviour of concrete (Wittmann, 1993). Moisture diffusion during drying causes non-linear shrinkage strain distributions throughout the thickness of the concrete sample, leading to stresses due to loads and boundary constraints (Idiart, 2009). Experiments performed over the years have consistently demonstrated that the deformations measured at the surface of the concrete block samples are greater than when measured at the centre, as can be observed in Figure 5b (Wittmann, 1993). Thus, the accurate placement of strain measurement points is essential in obtaining reliable drying shrinkage results.

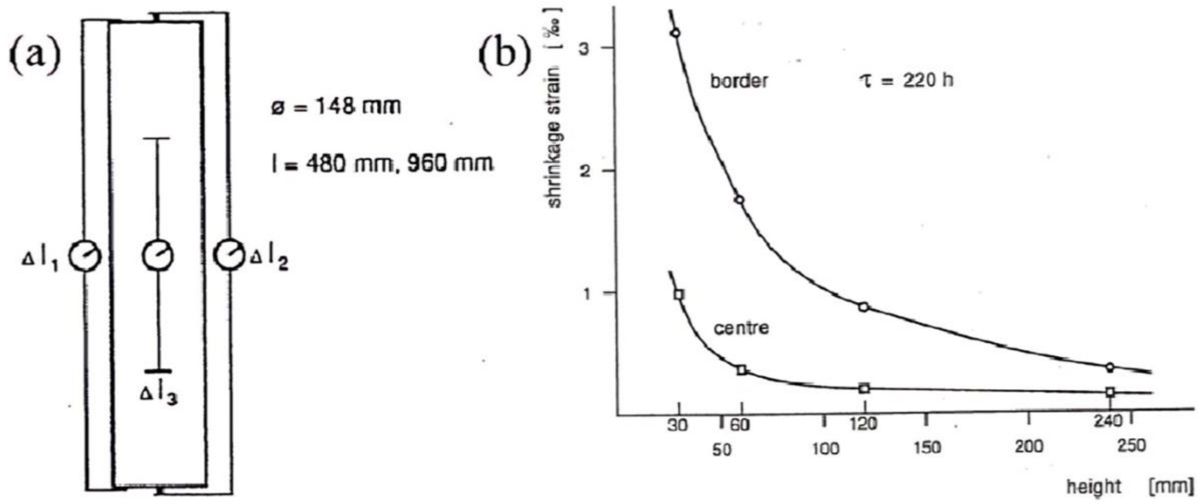

Figure 5: a) Different strain measurement possibilities in a drying shrinkage test b) Relation between the height of concrete specimens and the measured longitudinal strains at the border/centre of the samples

To acquire an approximation of the long-term drying shrinkage curve, it is crucial to select an optimum duration for the drying shrinkage tests of concrete blocks. Previous Canadian data from laboratory and onsite experiments were referenced for selecting the appropriate duration. These previous studies neglected the effect of mortar joints; however, this effect must be accounted for to enable the use of simplified numerical modelling techniques e.g., those based on material homogenization. By considering the mechanical interaction between blocks and mortar, it is intended to get insight into the moisture-induced shrinking of modern concrete masonry assemblies. The following two Canadian studies, which employ similar methods to those selected for this research as described below, were used for reference:

- Drysdale & Khattab, 1995 – twenty-four hollow 20 cm concrete block tests were performed over a period of two and a half months, roughly 80 days, in the McMaster University laboratory. The drying shrinkage of each block was measured along the long horizontal axis using four strain indicators on each of the two face shells in accordance with the ASTM C426-94 guidelines (1994 edition), as shown in Figure 6. The blocks were initially soaked in water for three days at room temperature, and strain readings and weights were taken after draining the specimen to a saturated surface dry condition. The blocks were then air-dried in a room that was humidity- and temperature-controlled, with regular measurements of shrinkage and weight taken during this period. After reaching a stable shrinkage value and weight at 2½ months, final readings and weights were taken by oven-drying the blocks. (Drysdale & Khattab, 1995).

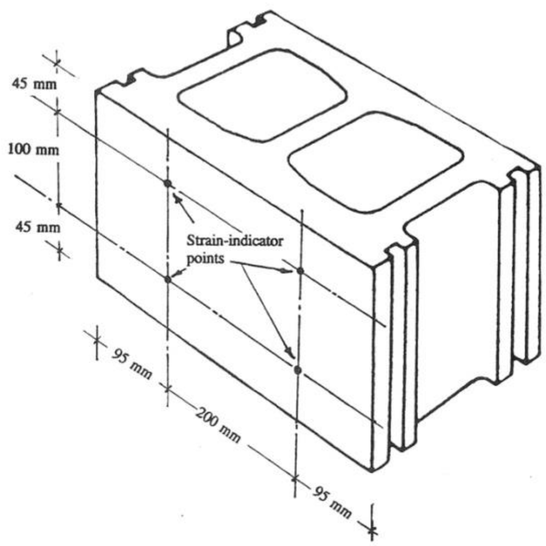

Figure 6: Drysdale and Khattab (1995) experimental program: Position of stain indicator points on the face shell of a concrete block

- Kuzik, Elwi, & Hatzinikolas, 1999 – five 20 cm hollow concrete blocks were subjected to testing, following a procedure that closely resembled that of Drysdale and Khattab (1995), at a temperature of 22°C and a 'very low' relative humidity, although the exact value was not reported. The researchers also reported on the differential movement in cavity-walls of a full-scale clock tower, measuring 21 meters tall, located in Edmonton, Alberta, and exposed to the outdoor environment (see Figure 7). DEMEC points were utilized to measure the differential movements between the block and brick wythes for each wall. In parallel with the field test monitoring, 5 concrete blocks were taken from the clock tower to the laboratory for monitoring. These specimens were also left in a room with a controlled temperature and relative humidity to measure the dimensional changes, similar to the method used by Drysdale and Khattab (1995). It is interesting to note that both the lab-constructed blocks and those taken from the field exhibited comparable shrinkage behaviour, with only marginal differences. Therefore, only the results obtained from the lab-constructed specimens were utilized for comparison in this thesis paper. (Kuzik, Elwi, & Hatzinikolas, 1999).

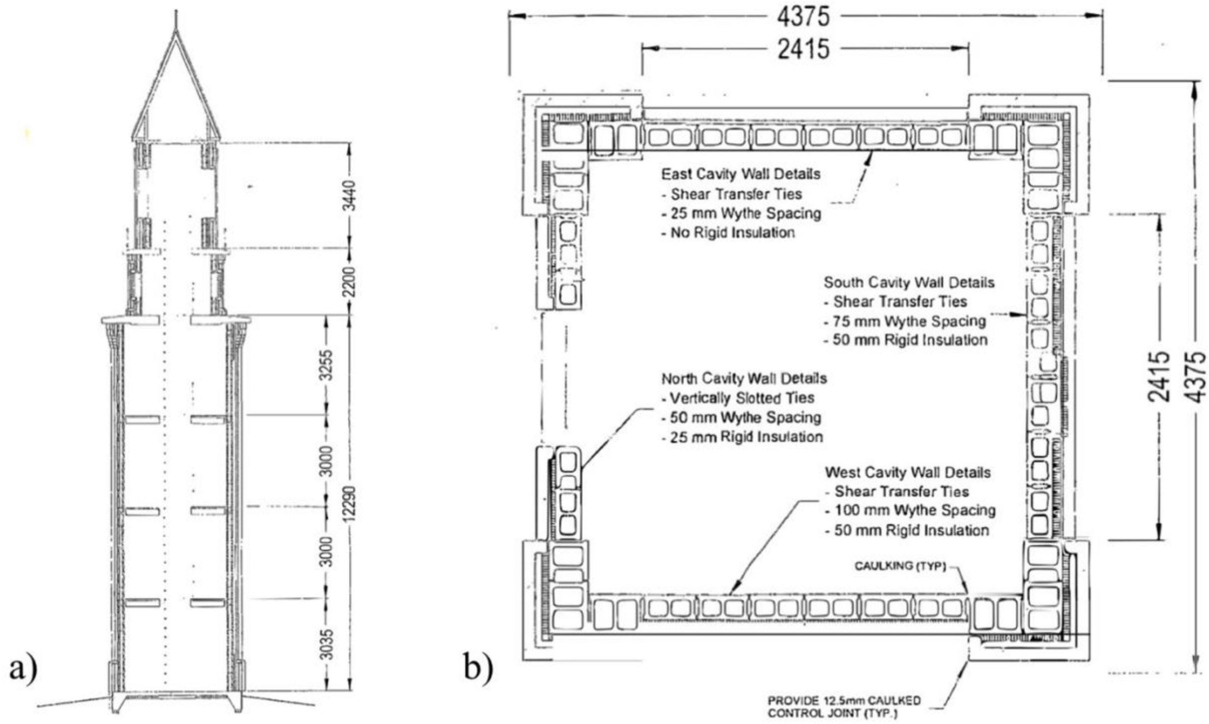

Figure 7: Kuzik et al. (1999) experimental program:
a) Elevation of Perron Clock Tower b) Cross-section of instrumented region of tower

In Figure 8 and Figure 9, the specimens tested by Drysdale and Khattab (1995) and Kuzik et al. (1999) are depicted, and the experimental results are plotted. These normalized graphs were produced by taking the reported ultimate drying shrinkage for each specimen in both studies and then plotting the drying shrinkage strain for each measurement as a percentage of the ultimate shrinkage strain.

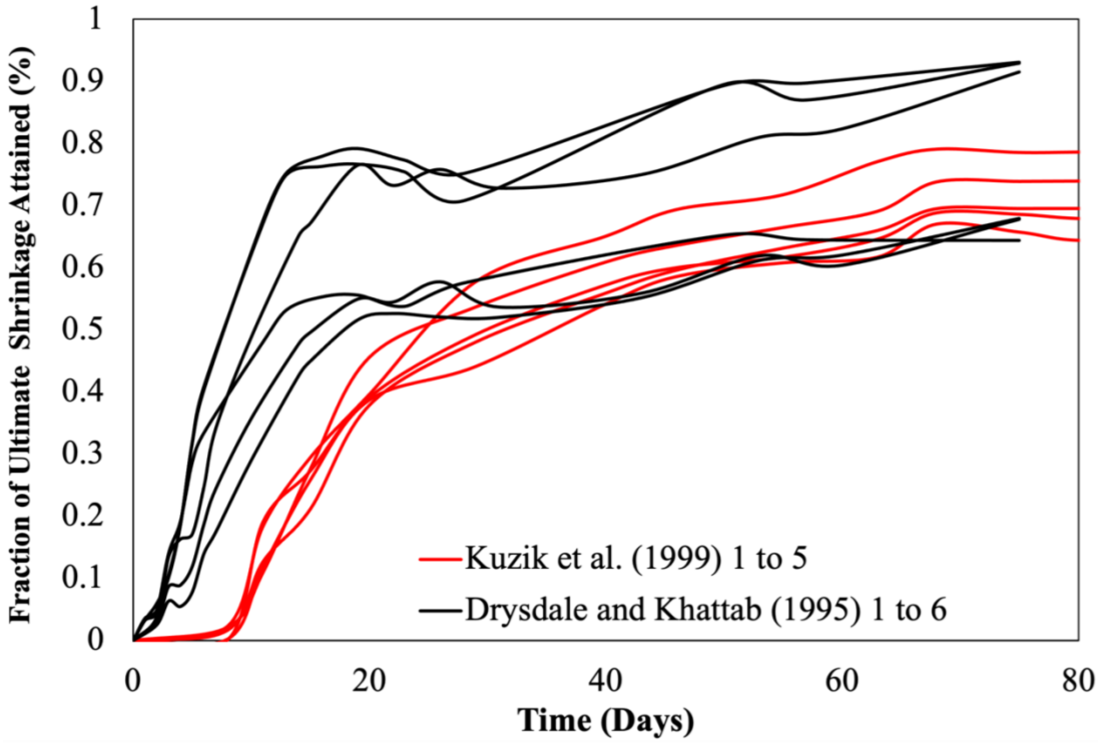

Figure 8: Results from Drysdale and Khattab (1995) and Kuzik et al. (1999) up to day 80

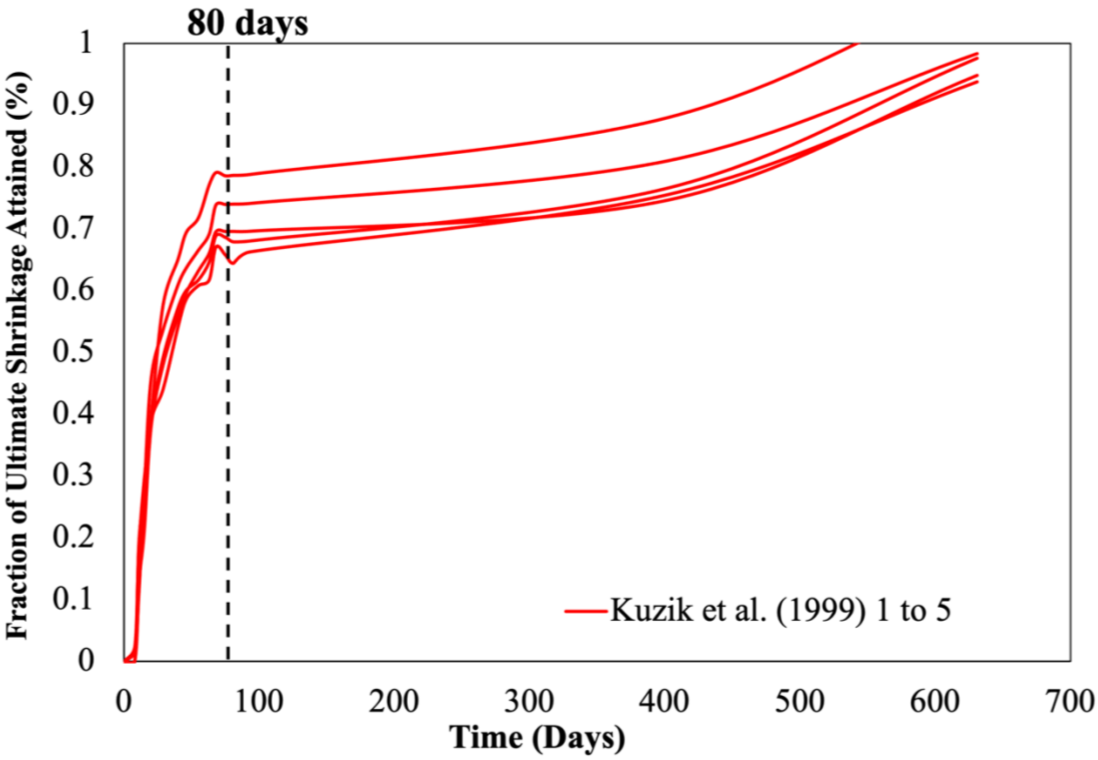

Figure 9: Results from Kuzik et al. (1999) up to day 631

Drysdale and Khattab (1995) demonstrated that drying concrete blocks to a certain moisture content, expressed as a percentage of total absorption, has little influence on shrinkage. Instead, a better correlation between shrinkage and water content is achieved when expressed as an absolute value. On the other hand, Kuzik et al. (1999) provided the average shrinkage value obtained on day 1310, while noting that the shrinkage achieved on day 631 was consistent with the maximum value specified in the CSA S304.1-94 provisions.

The block wythe shrinkage in the cavity-walls reported by Kuzik et al. (1999) was also in agreement with the shrinkage determined in the laboratory experiments. Such data analysis helped determine the optimal duration of long-term drying shrinkage for step 1 of a proposed procedure that would yield meaningful results in a reasonable timeframe. Previous experiments, including Kuzik et al.'s (1999), lasted over three and a half years, which is not practical for industry and applied research priorities. Figure 8 and Figure 9 show that shrinkage percentages plateaued at around 80 days, with a slow increase to ultimate shrinkage over hundreds of days. Therefore, the 80-day period was chosen (84 days or 12 weeks in this study) since it had the largest gradient of linear shrinkage before deformation became negligible. However, laboratory data on shrinkage behaviour only pertains to concrete blocks, and it is unknown if mortar joints affect masonry assembly behaviour. Additionally, the available laboratory data is outdated and may not reflect the actual moisture response of modern masonry, considering advancements in materials, manufacturing processes, and construction practices. For example, the increasing trend of sustainable construction in the last 2 decades has led to the use of recycled materials and low-carbon alternatives in masonry, which can significantly impact the behaviour of concrete and mortar. Thus, to obtain accurate information on modern masonry behaviour, re-evaluation of old data and new experiments are necessary.

Drying shrinkage, which is expressed as a percentage of the dry length, is determined by measuring the difference in length of a concrete block specimen that has been submerged in water and dried until it reaches a specified constant length. The change in size of the specimen is observed from a saturated to an equilibrium condition (American Society for Testing and Materials, 2006). Linear shrinkage of a concrete specimen is calculated according to ASTM C426-06 and is expressed as a percentage of the gauge length as shown in the equation below:

$$\boldsymbol{S = \left(\frac{\Delta L_x}{G}\right) \cdot 100}$$

$$\boldsymbol{\Delta L_x = \left(L_{I(73.4)} - R_{I(73.4)}\right) - \left(L_{x(73.4)} - R_{x(73.4)}\right)}$$

where:

$S =$ linear drying shrinkage, %

$\Delta L_x =$ change in the linear dimension of the specimen due to drying from a saturated to the length of the specimen at any time, x, in. (mm),

$G =$ test specimen gage length, in. (mm)

$L_{I(73.4)} =$ specimen length reading on saturated specimen, corrected for temperature, in. (mm),

$R_{I(73.4)} =$ accompanying reference bar length reading for L_I, in. (mm)

$L_{x(73.4)} =$ specimen length reading at any time x, corrected for temperature, in. (mm), and

$R_{x(73.4)} =$ accompanying reference bar length reading for L_x, corrected for temperature, in. (mm) (American Society for Testing and Materials, 2009).

Although the ASTM C426-06 specifies tests for determining linear shrinkage values of concrete masonry units, its inadequacies restrict the rapid shrinkage test to only provide the final value. Furthermore, there are no equivalent standards available for determining the linear shrinkage of masonry assemblies. Therefore, a two-step procedure is proposed in the following subsection as a new research direction.

1.5 Knowledge gaps and innovative research directions

To inform future masonry designs and meet more stringent sustainability goals in a changing climate, several research efforts have been undertaken to create advanced simulation methods and durability guidelines (Vandemeulebroucke, Defo, Lacasse, Caluwaerts, & Van Den Bossche, 2011; Lacasse, et al., 2018). However, to establish the implementation of these designs in building codes, a reliable foundation of experimental data is required, which is presently lacking. Currently, available tests on volumetric changes in masonry assemblies (differential movements due to clay brick expansion/ concrete block shrinkage are the leading cause of masonry cracking, reducing durability) due to moisture variations (correlated to precipitation and temperature swings, affected by climate change), which are the leading cause of masonry cracking and reduced durability, are limited and mostly conducted decades ago or in-situ on old structures (Kuzik, Elwi, & Hatzinikolas, 1999; Shrive, Sayed-Ahmed, & Tilleman, 1997; Drysdale & Khattab, 1995; Lohonyai, Korany, & Gül, 2015). While more tests have been performed on complementary time-dependent masonry deformations, e.g. creep, cyclic temperature and freezing volumetric variations, the governing plastic phenomena seem to be mainly related to moisture (Drysdale & Khattab, 1995; Shrive, Sayed-Ahmed, & Tilleman, 1997; Dias, 2002; Zhou, Carmeliet, & Derome, 2020). In 1999, data extracted from the monitoring of a cavity-wall tower in Alberta showed that differential movements among inner and outer wythes were dominated by loadbearing concrete unit shrinkage, while that of mortar mitigated brick expansion; albeit informative, these findings are not necessarily valid for modern materials (Kuzik, Elwi, & Hatzinikolas, 1999). Although CSA technical reports suggest the use of wider cavities to mitigate climate change effects, the required structural implications and design modifications to key components remain unclear and have not been investigated recently. The most recent tests correlating cavity width and tie coupling capacity were conducted 30 years ago, despite being critical for complying with the objective-based provisions of the National Building Code of Canada (Sparling, Palermo, & Khan, 2021; Hatzinikolas, Longworth, & Warwaruk, 1982).

This thesis aims to fill the research gaps mentioned above by presenting innovative directions. Through new experimental testing of the shrinkage behaviour of concrete masonry, the expected outcome is to quantify the impact of temperature and moisture swings induced by climate change on new cavity-wall masonry constructions. Currently, the design of cavity-walls in Canada relies on outdated drying shrinkage data that only refers to individual concrete blocks. To gather new insights into the moisture-induced shrinkage of modern concrete blocks and account for the mechanical interaction between units and mortar, this paper presents a novel two-step testing method for unconstrained mortared concrete masonry prisms and discusses preliminary results as well as some new results. The two-step procedure mixes two approaches originally conceived for units, i.e. the one developed by Drysdale et al. (1995) (slow method, step 1) and that recommended in ASTM C426-06 (slow method, step 2). The combination of these procedures allows for shrinkage-time curves to be inferred over an adequately long period for numerical analysis purposes in step 1, while also allowing for the ultimate drying shrinkage of the specimens – needed for most design applications – to be estimated in step 2. At a later stage in the larger project, numerical simulations (via Discrete Element Method, DEM) will also be conducted to extend experimental findings to additional geometries, material properties and loading conditions. The inferred data obtained from this research will guide the development of suitable climate-adapted cavity-wall designs that will be translated into design guidelines updating reference masonry standards (CSA A370-14, CSA A165.1-14, CSA S304-14). Implementations of climate-adapted codes will lead in the long-term to more resilient and sustainable built environments, supporting Canada's commitments under e.g., the *Paris Agreement*, the *United Nation's Agenda of Sustainable Development*, and the *Sendai Framework for Risk Reduction*.

2 EXPERIMENTAL WORK

2.1 Geometrical characteristics and construction of tested specimens

For the construction of the masonry doublets (2 units) and triplets (3 units), standard hollow concrete blocks were used, and high-strength commercial mortar (QUIKRETE Mason Mix) was used to join the units. The concrete blocks used for the experiment are representative of the most commonly used blocks in the field. QUIKRETE Mason Mix was also specifically selected as it follows standardized formulation and manufacturing processes, ensuring that the product represents a typical mortar mix commonly used in the construction industry. A total of 11 single units, 4 doublets, and 4 triplets were constructed for testing purposes. In addition to the concrete masonry units, 5 mortar specimens were also built to be tested separately. The details of each specimen to be tested for drying shrinkage are provided in Table 3.

Table 3: Geometrical characteristics of concrete single units, doublets, triplets, and mortar prisms

	Specimen			
Characteristics	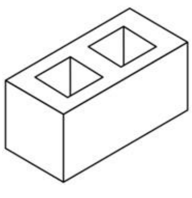 x 11	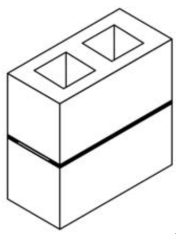 x 4	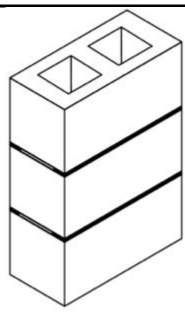 x 4	 x 5
Width (cm)	19	19	19	2.5
Length (cm)	39	39	39	2.5
Height (cm)	19	39	59	28.5
Compressive strength (MPa)	15	15	15	—

The dry mortar used is a pre-blended mixture of cement and sand, which meets the N, S, M requirements specified in ASTM C270-19 and C1714-19 as Type S Mortar. According to ASTM C270-19, the design average minimum 28-day compressive strength of Type S mortar is 1,800 psi (12.4 MPa). To prepare the mortar mixture, 80 lb (36.2 kg) of mortar and 4.7 L of water were used, and minor variations in the water volume of up to 1.9 L were acceptable to adjust the workability. These proportions were sufficient to create several doublets, triplets, and prisms and were appropriately scaled to produce larger or smaller batches of mortar. The batches of mortar were mixed in a mixing apparatus for a minimum of 5 minutes until a firm, workable consistency was achieved. The ideal consistency was determined when a 0.5 in (13 mm) layer of mortar adhered to the trowel while being held in a nearly vertical position. The fine aggregates in the mortar were allowed to saturate for 3 to 5 minutes without being disturbed. A flow test was performed for each mortar mix to maintain the desired workability and flow characteristics of the mortar throughout the experiment. For the mortar mixes used for the experiment, the primary focus was on achieving consistency rather than targeting a specific strength during the contrasting process. By following the guidelines outlined in ASTM C1437-20, the desired range for flow was approximately 105-115%.

To assemble the specimens, a 1 cm thick layer of mortar was evenly spread on the face-shell area of the hollow concrete blocks, as illustrated in Figure 10, with the help of a wooden frame mould. The blocks were stacked on top of each other and levelled each time. After approximately one hour of drying, when the mortar joints between the units were "thumbprint hard," they were tooled to achieve a smooth surface. The units were then cured in a polyethylene sheet for 7 days and then in the curing chamber for an additional 21 days. For the new testing batch, to avoid excessive transportation and the risk of breakage, the specimens were cured using humidifiers placed under the polyethylene sheet to recreate the curing chamber conditions.

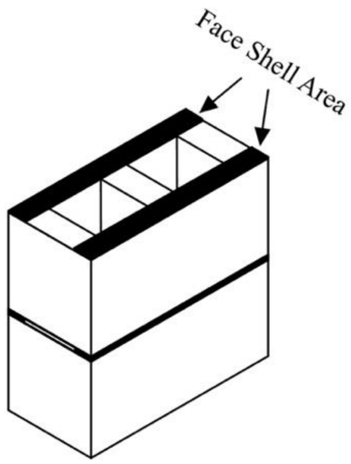

Figure 10: Mortar distribution on face shell area of concrete masonry blocks

Figure 11: Construction of tested specimen:
a) Mortar mixing, b) Block levelling, c) Casted doublets, d) Casted triplets,
e) Specimen curing, f) Mortar flow test, and e) Mortar prisms

The construction process to mould the mortar specimens as well as to assemble the concrete specimens is shown in Figure 11. The mortar specimens were constructed in accordance with ASTM C596-18, using the same proportion of water to mortar as described for the doublets/triplets. The mixture was moulded and cured for 24 ± 0.5 hours inside the mould, followed by an additional 24 ± 0.5 hours outside the mould within a curing chamber. After that, the specimens were cured in an immersion tank of lime-saturated water for 48 hours and then blotted with a damp cloth to achieve a surface-saturated dry state before commencing the drying shrinkage procedure.

The specimens were constructed in two different batches, using blocks from different palettes. Table 1 provides an overview of the number of specimens cast and used for all the testing, including both preliminary and new batches.

Table 4: Number of concrete single units, doublets, triplets, and mortar prisms used for testing

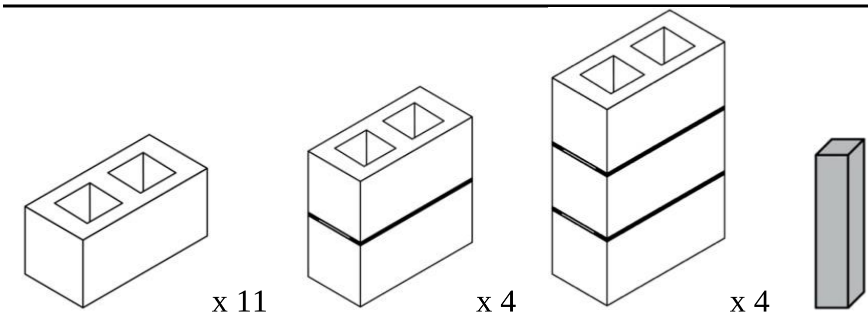

	Number of specimens			
Testing	x 11	x 4	x 4	x 5
Preliminary step 1	2	2	2	5
New step 1	2	2	2	—
Preliminary step 2	2	—	—	—
New step 2	5	—	—	—

The first batch was cast to obtain preliminary results and to ensure that the experimental research was on track and aligned with previous studies. In the preliminary tests, the researchers likely tested the infrastructure and identified any potential issues with the experimental setup or procedures. The second batch of specimens was then cast with improved procedures and optimized data collection frequency to obtain more precise and comprehensive data. The modifications made to the casting process and data collection were based on the findings from the preliminary tests, which helped to establish a baseline and identify any potential issues.

To prepare the single units, doublets, and triplets for steps 1 and 2, first, the gauge plugs must be affixed with epoxy glue to the surface of the specimen. As research has shown that deformations measured at the surface of units are greater than those at the center (as discussed in section 1.4), it is expected to get larger deformations along the longitudinal axis when measuring on the face shell than measuring at the center of the ends using a comparator. To allow for maximum strain readings, the layout of the gauge plugs on a unit is shown in Figure 12. According to section 6.2 of ASTM C426-06, the gauge plugs should be positioned in pairs parallel to the center line in each of the two opposite faces of the specimen.

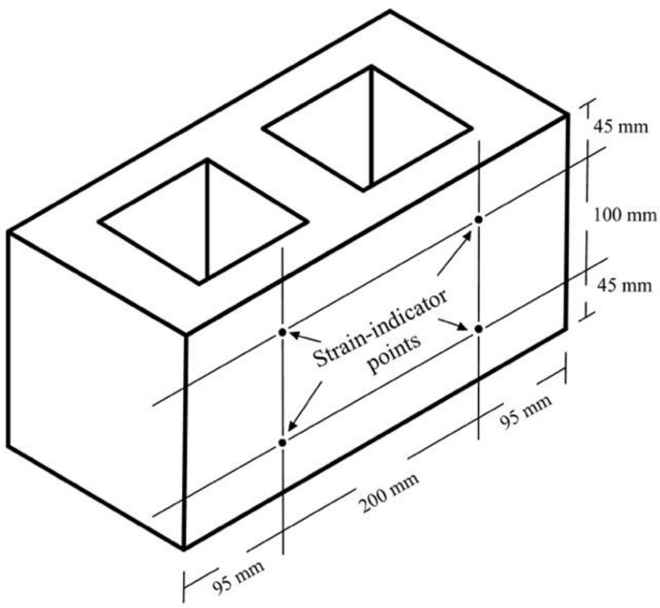

Figure 12: Gauge plugs layout for each face of a single concrete masonry unit

Every single block has 8 plugs, each doublet has 16, and each triplet has 24. For a single block, the exact dimensions shown in Figure 12 can be followed. However, for doublets and triplets, to maintain consistency, it was crucial to ensure that the distance between DEMEC points across the mortar joints was exactly 100 mm. Figure 13 shows the final assembled specimens along with the placements of gauge plugs.

a) b) c)

Figure 13: Gauge plugs placement on a) Single block, b) Doublet, and c) Triplet

In addition to the concrete blocks, the study also examined the behaviour of mortar prisms under different conditions. To prepare the mortar specimens for steps 1 and 2, the specific ASTM C490-07 procedure. First, the specimens need to be cured for 24 ± 0.5 hours within their moulds inside a curing chamber. After this initial curing period, the specimens are taken out from their moulds and immersed in a lime-saturated water tank for 48 hours. This immersion process is important to ensure the specimens are fully saturated with water before being subjected to air-drying conditions. After 72 ± 0.5 hours, when the curing process is complete, the mortar prisms are taken out from the water tank and blotted to achieve a surface-saturated dry condition. At this point, an initial comparator reading is taken for each specimen to establish a baseline for subsequent measurements. Once the initial readings are taken, the mortar prisms are moved into the air-drying fridge to begin the air-drying process.

2.2 Experimental framework and infrastructure

The prime objective of this experiment is to infer time vs micro-strain drying shrinkage curves for concrete masonry, vital for substantiating the numerical analyses planned for the larger research program, and to identify climate-adapted design requirements for movement joints and shelf-angles in case of wider cavities. The new testing methodology involves combining two approaches originally designed for units—the slow method (step 1, modified from Drysdale and Khattab (1995)) and the ATM C426 quick method (step 2)— applied to unrestrained concrete masonry prisms in a two-phase process. ASTM C596-18 was used for testing mortar samples.

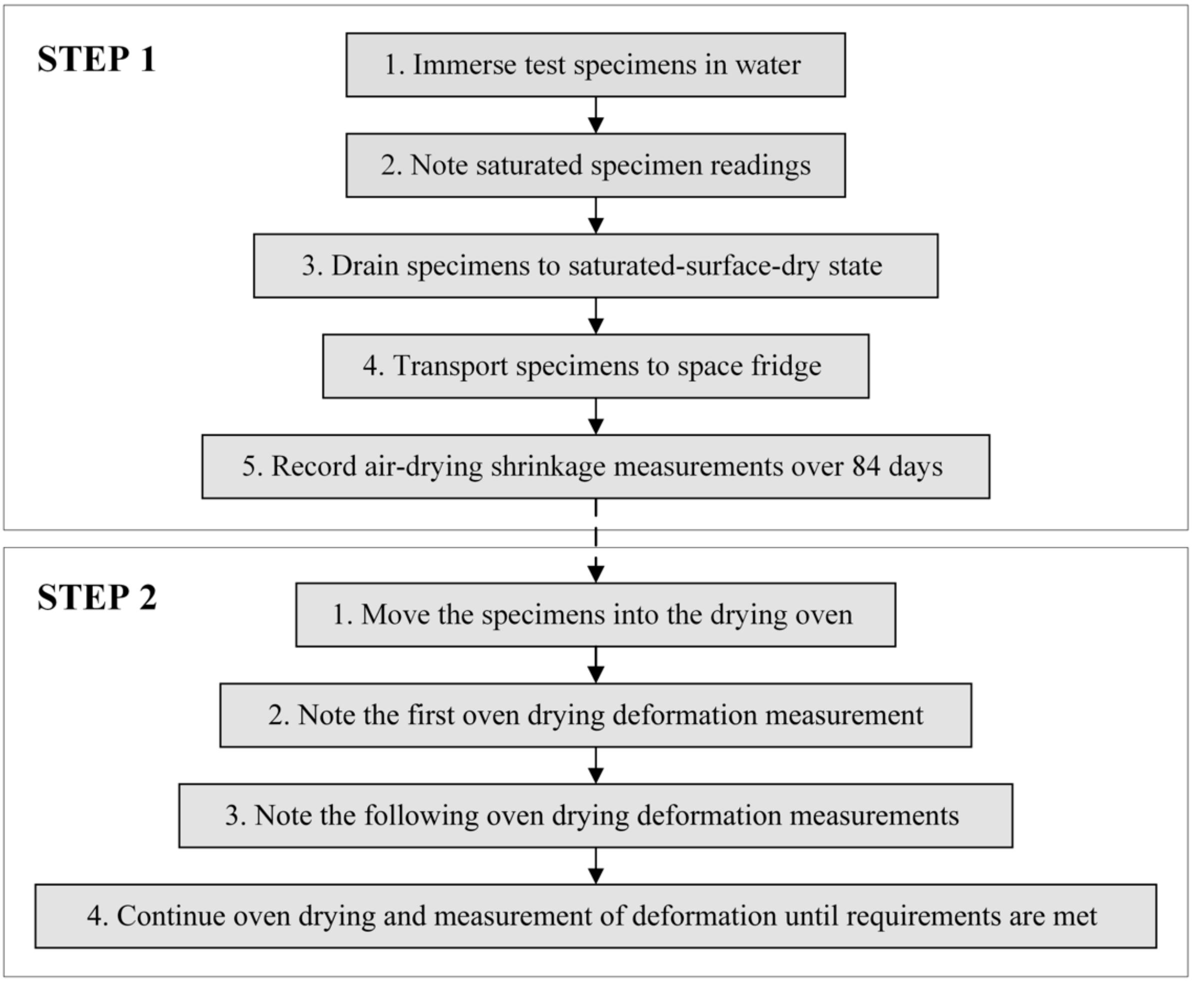

Figure 14: Procedure overview of step 1 and step 2

Figure 14 represents a general overview of the experimental framework for both step 1 and step 2. The figure illustrates the main steps involved, which were formulated based on previous research, as discussed earlier. For a more detailed understanding of the testing procedure, the following subsections provide a step-by-step explanation of both step 1 and step 2. These subsections detail the exact apparatus and testing conditions used for each step, including the type of specimen, the duration of testing, the environmental conditions, and the specific apparatus used to monitor the specimens' deformations.

The two-step procedure, which required several specifications to be followed, was employed to evaluate the drying shrinkage behaviour of the concrete masonry. In step 1 (refer to section 2.4 for a detailed procedure), prisms in saturated surface dry conditions were left to dry at 21 ± 2°C and relative humidity of 45 ± 5% for 85 days; deformations were periodically monitored. In step 2 (refer to section 2.5 for a detailed procedure), prisms were placed in a drying oven at a temperature of 50°C and relative humidity of 17%, until their weights stabilized. This combined procedure allowed us to infer the shrinkage-time curves for a reasonably long time (84 days - characterized by the largest deformation gradient, see section 1.4) while estimating the ultimate value through rapid drying. To compare and update values provided in CSA A165.1-14 as well as correlate unit shrinkage and relative humidity, the same tests were performed on blocks and mortar samples; a relevant and immediate contribution to this CSA standard.

The drying shrinkage tests were carried out in the Jamieson Structures Laboratory at McGill University utilizing all the equipment and apparatus shown in Figure 15. The experimental infrastructure used equipment and apparatus that were in accordance with the ASTM C426-06 requirements for testing concrete masonry.

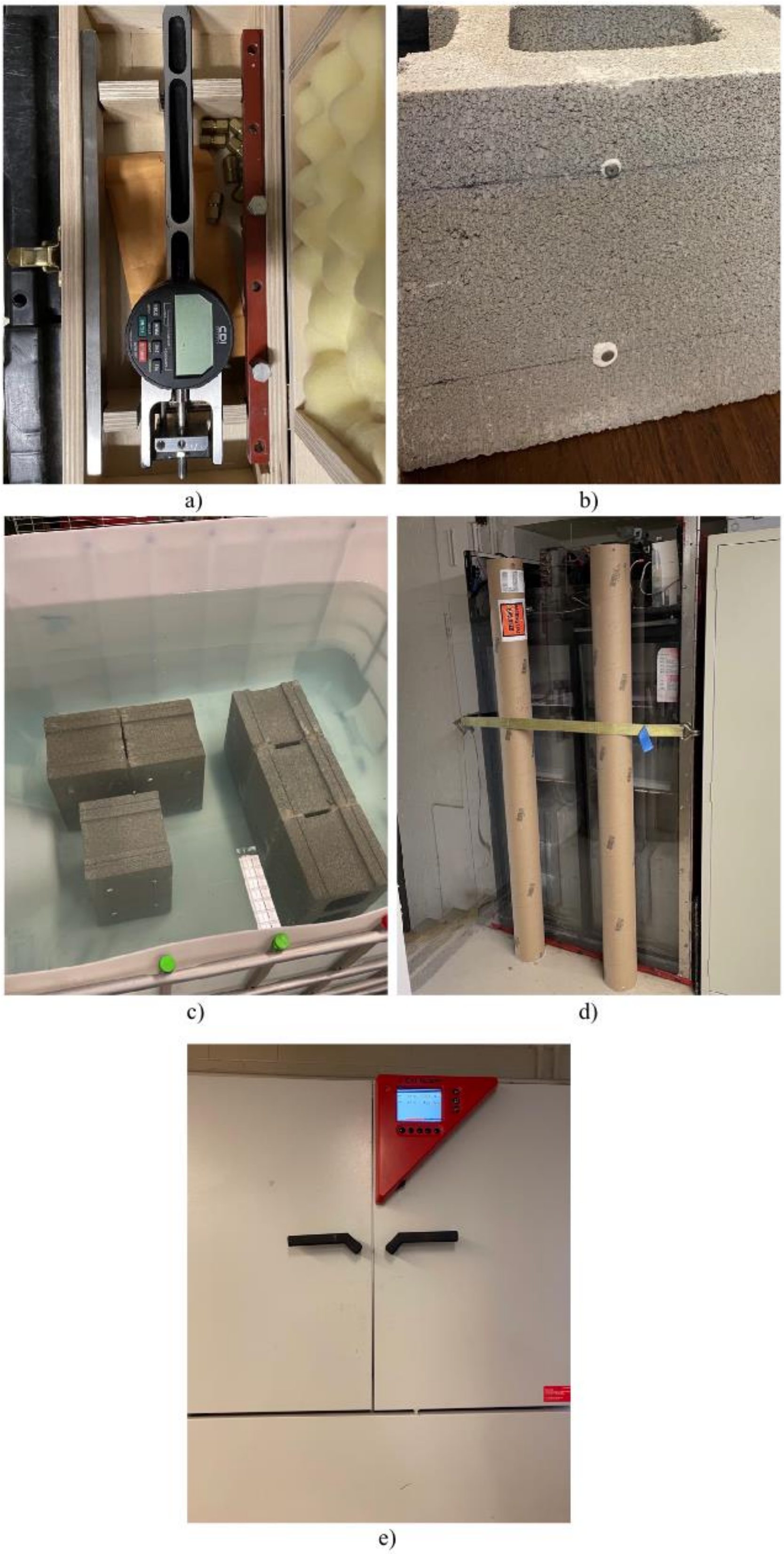

Figure 15: Equipment and apparatus: a) Multi-length strain gauge set, b) DEMEC plugs, c) Immersion tank, d) Controlled fridge, e) Airtight drying oven

A multi-length strain gauge set, which included a strain gauge with a sensitivity of 0.0001-inch and a standard reference bar to ensure accuracy, was used as seen in Figure 15a. The gauge plus glued with epoxy on the surface of the specimens were specifically DEMEC plugs that are 3/8 inch in diameter and ½ inch in thickness as depicted in Figure 15b. Figure 15c displays the immersion tank in which the specimens were submerged in water maintained at 23 ± 1.1ºC. For air-drying specimens, a fridge controlled at 22 ± 1 ºC and 42 ± 4% relative humidity was used as depicted in Figure 15d. Figure 15e shows the airtight drying oven with a constant uniform temperature of 50 ± 0.9ºC used. Finally, the specimens were cooled at a temperature of 23 ± 1.1ºC in a cooling chamber, which allowed them to reach a stable temperature before further testing. The temperature and relative humidity levels of all apparatus were constantly monitored throughout the experimental research. This was done using the Govee WiFi thermometer hygrometer H5179 smart humidity temperature sensor, which allowed for accurate and continuous monitoring. In addition, the apparatus also had direct readers to confirm that the temperature and relative humidity remained within the specified range.

2.3 Step 1

A total of 6 months were dedicated to work on concrete masonry linear drying shrinkage preliminary tests on unrestrained masonry prims. Once the preliminary data showed accurate trends that align with the previous studies, the collection of new results also began, and another 2 months of data collection was done to provide results for this thesis paper. It's worth noting that all the tests are still ongoing and will last another year to collect more data.

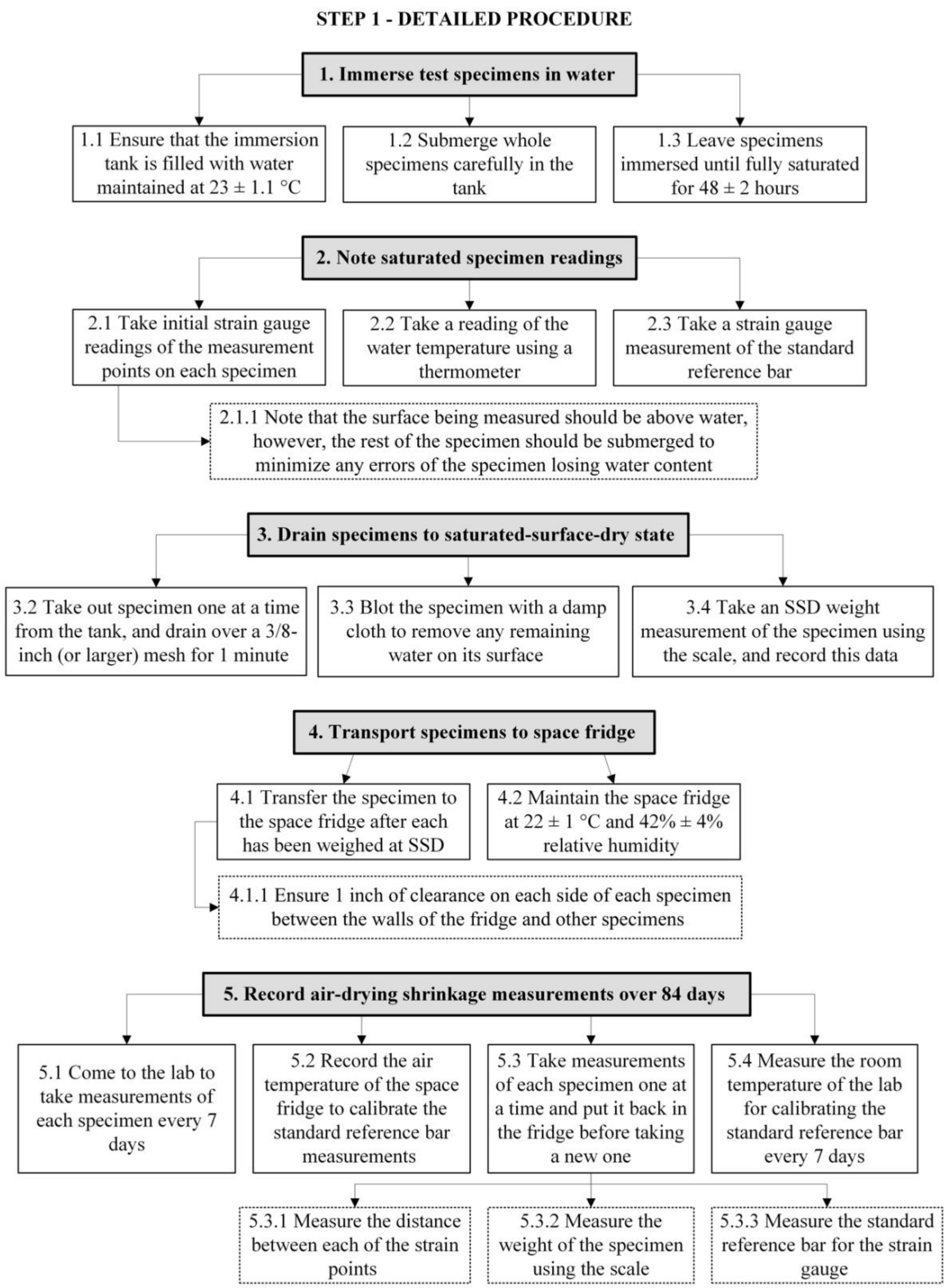

Figure 16: Detailed procedure of step 1, the slow method

Tests were carried out according to a two-step procedure (see section 1.5) mixing two approaches originally conceived for units. Step 1 is the slow method developed by Drysdale et al. (1995), and its procedure is explained in detail in Figure 16. It is assumed that specimens have already been assembled and are allowed to cure for 28 days. The gauge plugs should also be fully bonded to the specimen. For this first stage of the experimental research, both preliminary and ongoing new results were gathered. To obtain the preliminary shrinkage strain data, a total of two single blocks, two doublets, and two triplets were used. For the new results, the same number of specimens were used, but with blocks coming from a different palette.

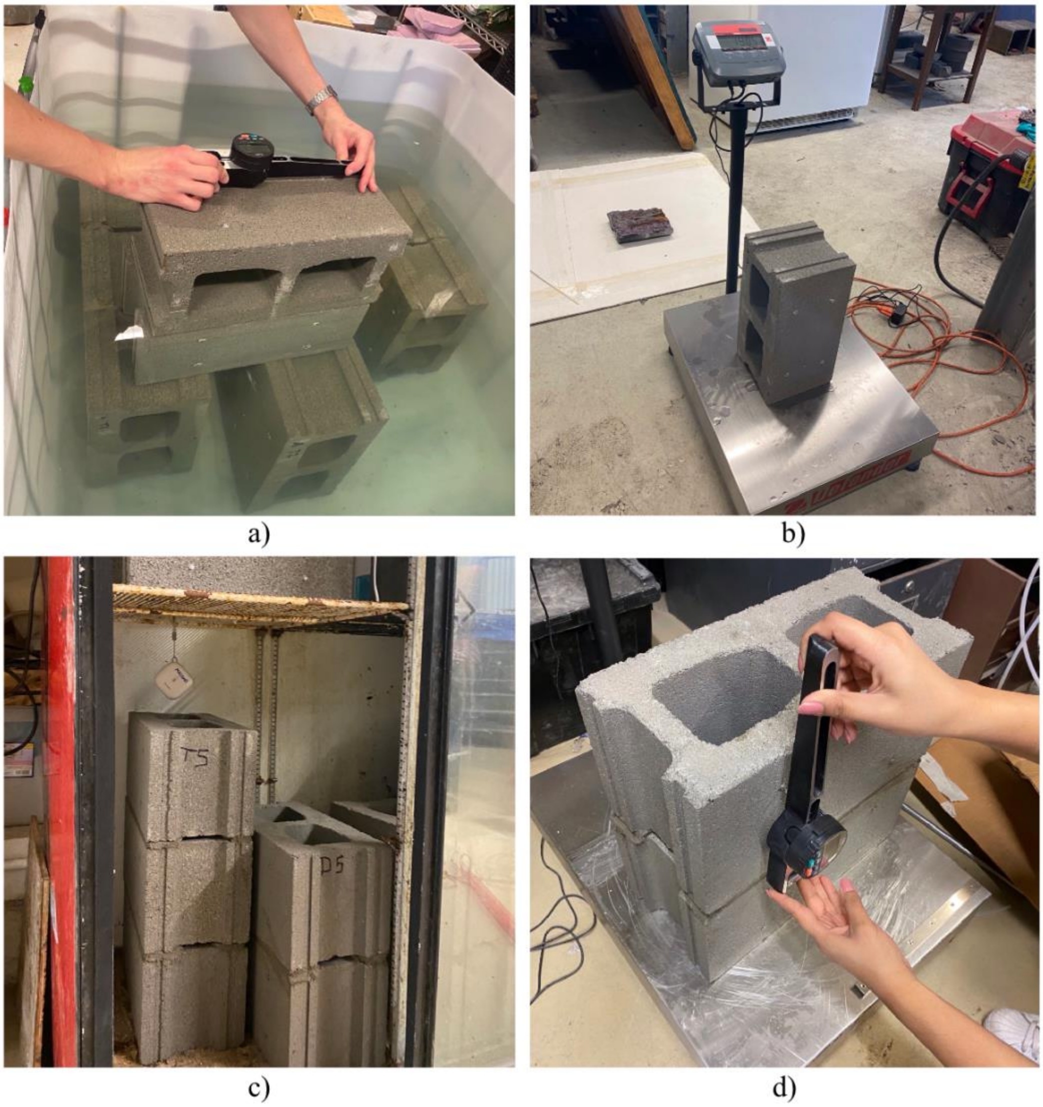

Figure 17: Step 1 experiment: a) Initial surface saturated strain reading, b) Initial weight reading, c) Specimens drying inside the fridge, d) Weekly deformation reading

A brief summary of the implementation of step 1 is reported in the bulleted list below and shown in Figure 17:

1. specimens are treated per ASTM C426-06 to reach saturated surface dry moisture conditions, with measurements of strain (Figure 17a) and weight (Figure 17b) taken.
2. specimens are left to dry for 84 days (or 12 weeks, i.e. the period with the largest gradient of linear shrinkage after which deformation becomes negligible, see (Menun, Das, Saad, Sparling, & Malomo, 2023)) at 22 ± 1ºC and 42 ± 4% relative humidity (Figure 17a).
3. mortar specimens were tested per ASTM C596-18, with weekly measurements of deformations using a DEMEC system over the 84-day process and of weight (Figure 17d).

2.4 Step 2

The procedure for step 2, the rapid method developed by ASTM C426-06, is detailed in Figure 18. Step 2 only begins after the step 1 procedure of drying shrinkage has been completed. However, for the results presented in this paper, blocks were placed under surface-saturated dry conditions without undergoing the first step and were subjected to oven drying. By conducting step 2 without the initial step 1, a comparison can be made between the ultimate shrinkage results obtained from the rapid drying method in an oven and the slower drying method in a fridge. By comparing the results obtained under these two different conditions, it is possible to determine if there are any significant differences in ultimate shrinkage. Both preliminary and ongoing new results have been collected for step 2, just like in step 1. The preliminary shrinkage strain data were obtained using two single blocks. For the new results, five single blocks from a different palette were utilized.

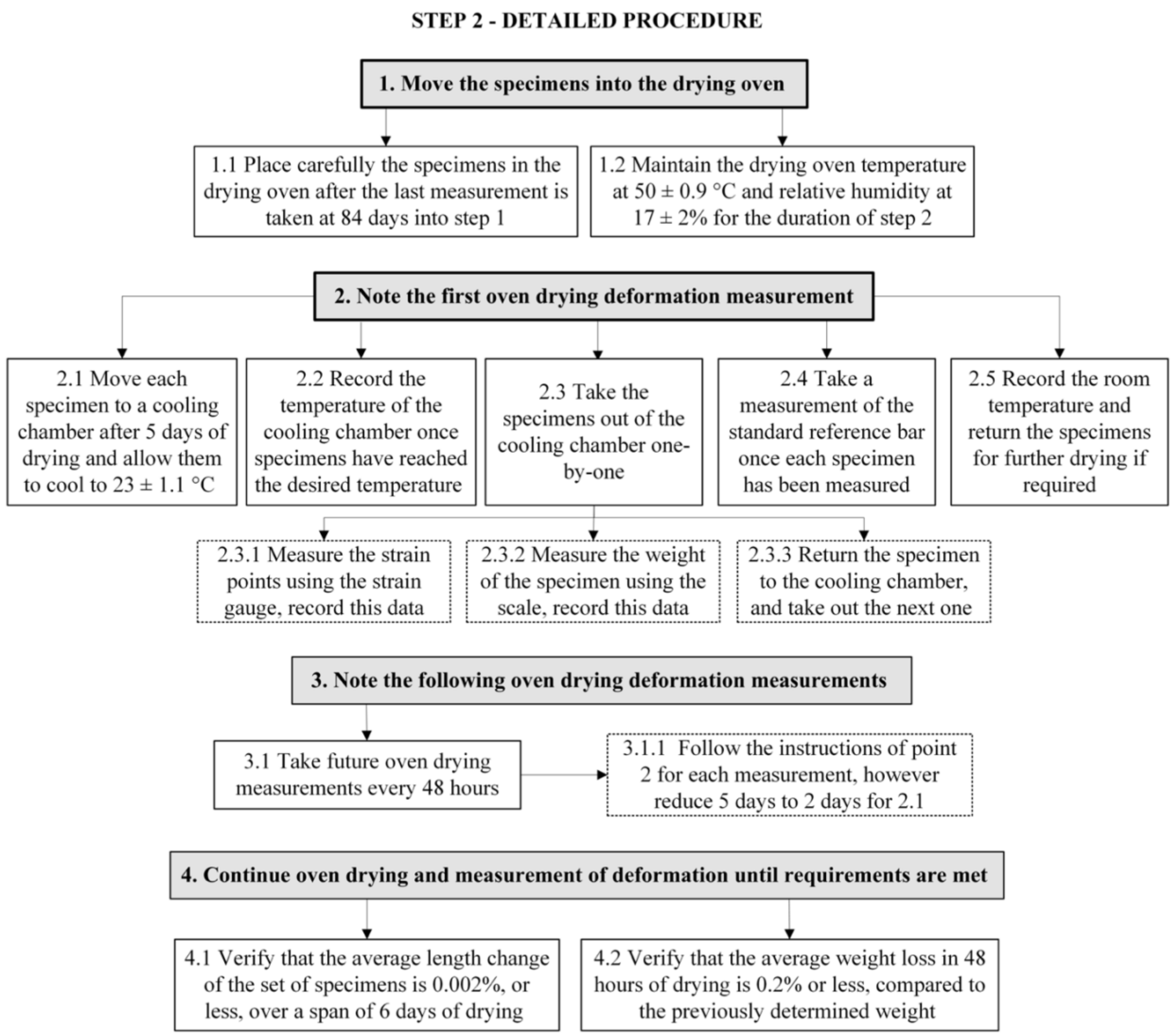

Figure 18: Detailed procedure of step 2, the rapid method

Step 2 is summarized in the list below and shown in the following Figure 19:

1. specimens are dried in an oven at 50 ± 0.9ºC and 17 ± 2% RH (Figure 19a).
2. after cooling (Figure 19b), the weight and shrinkage strain variations are recorded (Figure 19c) until negligible variation.
3. strain gauge measurements are corrected based on temperatures and standard reference bar readings during this stage, following Section 8 of ASTM C426-99.

Figure 19: Step 2 experiment: a) Specimens drying in the oven, b) Specimens in the cooling chamber, c) Deformation reading

This two-step combined procedure enables the inference of shrinkage-time curves for a reasonably long time while estimating the ultimate value via rapid drying. To correlate these results with those of units and joints, the same tests were performed on blocks and mortar samples. Maximum moisture content was also measured for units, to compare inferred values with those provided in CSA A165.1-14 for linear shrinkage.

3 RESULTS DISCUSSION

3.1 Preliminary results of drying shrinkage environmental testing – Step 1

The drying shrinkage of concrete masonry prisms, doublets, triplets, and mortar was measured for a period of 10 weeks using a calibrated strain gauge. All raw data obtained during the experiment were normalized with respect to the initial length between gauge plugs at the first measurement. The normalized shrinkage strain (mm/m) over time (days) was then calculated and plotted to facilitate better analysis of the drying shrinkage trends. To further enhance the readability of the shrinkage strain plots, the horizontal and vertical measurements of the specimen faces were averaged separately. This approach provides a clear visualization of the shrinkage behaviour of each specimen, enabling a more detailed assessment of their performance over time. Each average was scrutinized by calculating the standard deviation to ensure the accuracy of the results. However, to prevent the curves from appearing too clustered, the standard deviation was not presented in the following graphs.

To start the research, the drying shrinkage of 5 mortar specimens was examined following the slow testing method (step 1). After curing, these specimens were placed in a fridge to maintain a constant temperature and relative humidity, and their measurements were taken with a strain comparator. Figure 20 illustrates the shrinkage of 5 mortar specimens over a period of 10 weeks. As shown in the figure, all 5 specimens exhibited similar drying shrinkage trends during the first 42 days, which is consistent with previous findings that used similar methods (Booya, Ghaednia, Das, & Pande, 2018; Gorospe, Dhaednia, & Das, 2019). This is an essential validation of the experimental methodology and reinforces the reliability of the data. However, technical difficulties were encountered when using the comparator device after day 42, and therefore the reliability of the data after that point may be limited. It is worth noting that the technical issues with the device have since been addressed and resolved, and therefore any new results using this device are unlikely to face the same limitations.

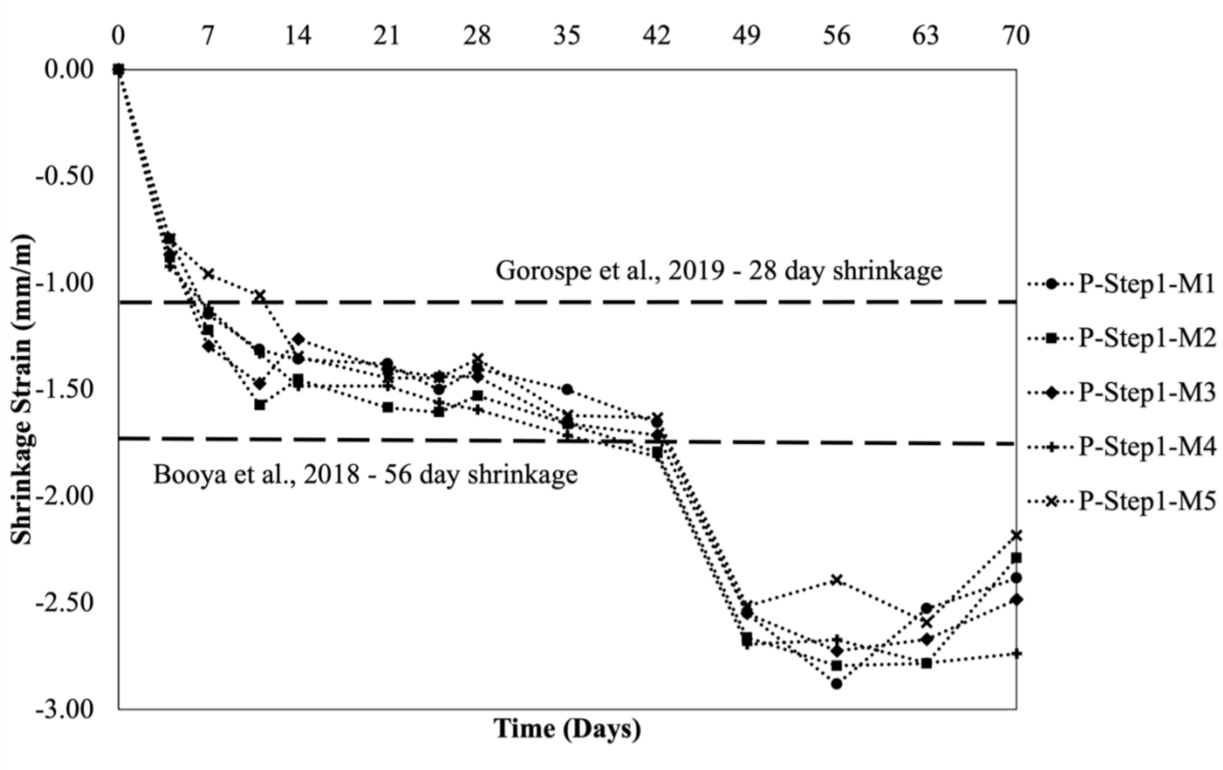

Figure 20: Shrinkage of ASTM C596 mortar specimens versus time, with benchmark from Booya et al. (2018) et Gorospe et al. (2019)

The preliminary results of weekly air-drying shrinkage measurements were obtained for 2 single concrete blocks, 2 doublets, and 2 triplets over a period of 70 days. After reaching the surface saturated dry condition, initial strain and weight measurements were taken of the specimens to serve as a reference for the normalization of the results. All the specimens were then left in a fridge at a controlled temperature and relative humidity. Weekly air-drying shrinkage measurements were taken using a calibrated strain gauge. Figure 21 illustrates the horizontal shrinkage results across the long dimension of faces. Although the blocks shrink a little slower than the masonry, these results indicate a minimal difference between the shrinkage trends. Notably, doublet 2 appears to have exhibited a relatively faster shrinkage rate than the other specimens. This difference is not minimal and will better be addressed with the new results of doublets (see section 3.3). At day 70, the single blocks have attained a shrinkage of -0.33 and -0.35 mm/m, while the doublets exhibit a shrinkage of -0.42 and -0.58 mm/m. The triplets exhibit a shrinkage of -0.34 and -0.44 mm/m. These preliminary results suggest that the shrinkage trends for the different specimens are relatively consistent, with only slight discrepancies observed in their shrinkage rates. It's worth noting that the slight discrepancy in shrinkage rates observed among the specimens could be attributed to variations in the manufacturing of the blocks or the construction process of the masonry specimens.

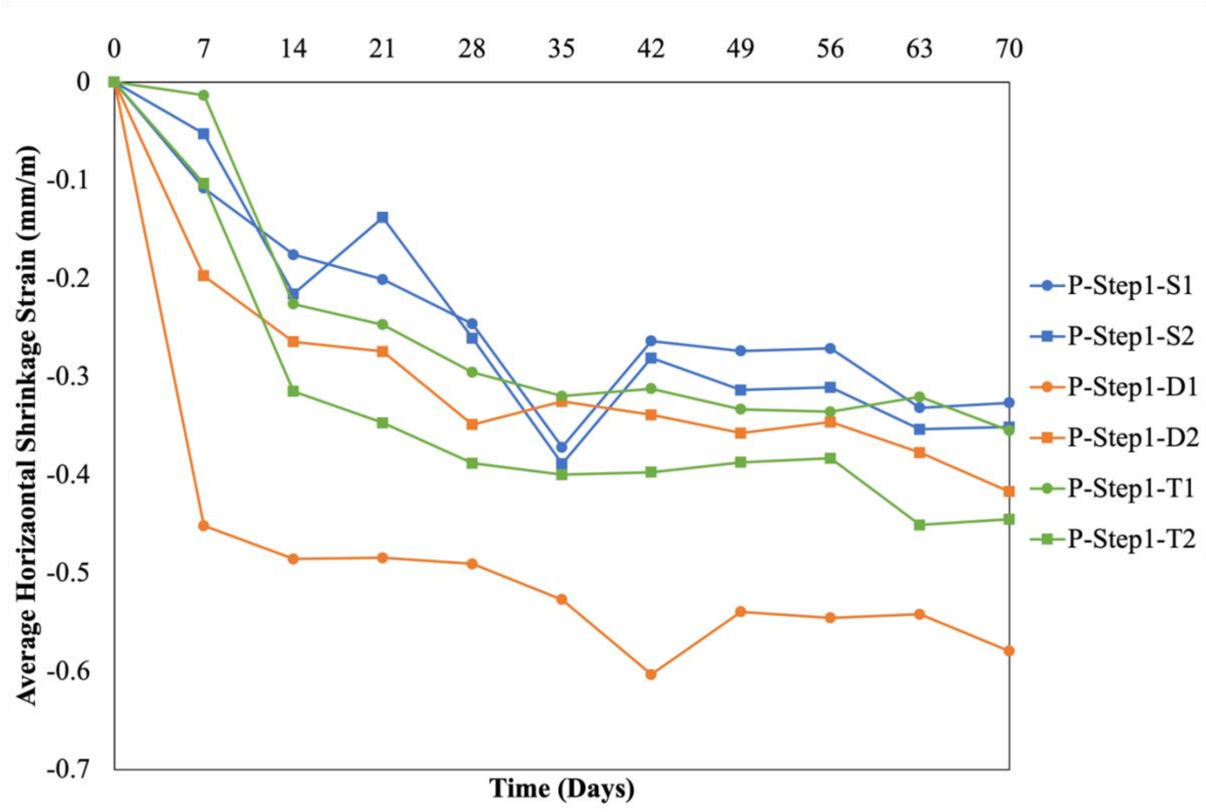

Figure 21: Average horizontal shrinkage for each specimen versus time – across the long dimension of faces

To ensure the accuracy of the results obtained, a comparison between the results of the two single blocks and the results of previous studies was made. The results of the masonry specimens could not be compared, as no previous studies have investigated this aspect. It is noteworthy that the preliminary results for single blocks demonstrate a strong correlation with previous shrinkage data reported by Drysdale and Khattab (1995) and Kuzik et al. (1999), as depicted in Figure 22. Despite some disparities, the shrinkage plots for each block seem to follow a similar overall trend. However, it is important to note that the average shrinkage identified in this study is lower than that reported in the previous research. This discrepancy may be attributed in part to the fact that the refrigerator's relative humidity in this study was slightly higher as it takes time to stabilize after the saturated blocks are placed in. It is important to note that these findings are preliminary, and further sample testing is required to establish statistical significance. Nevertheless, the strong correlation between the preliminary results and the previous research assures the accuracy of the results.

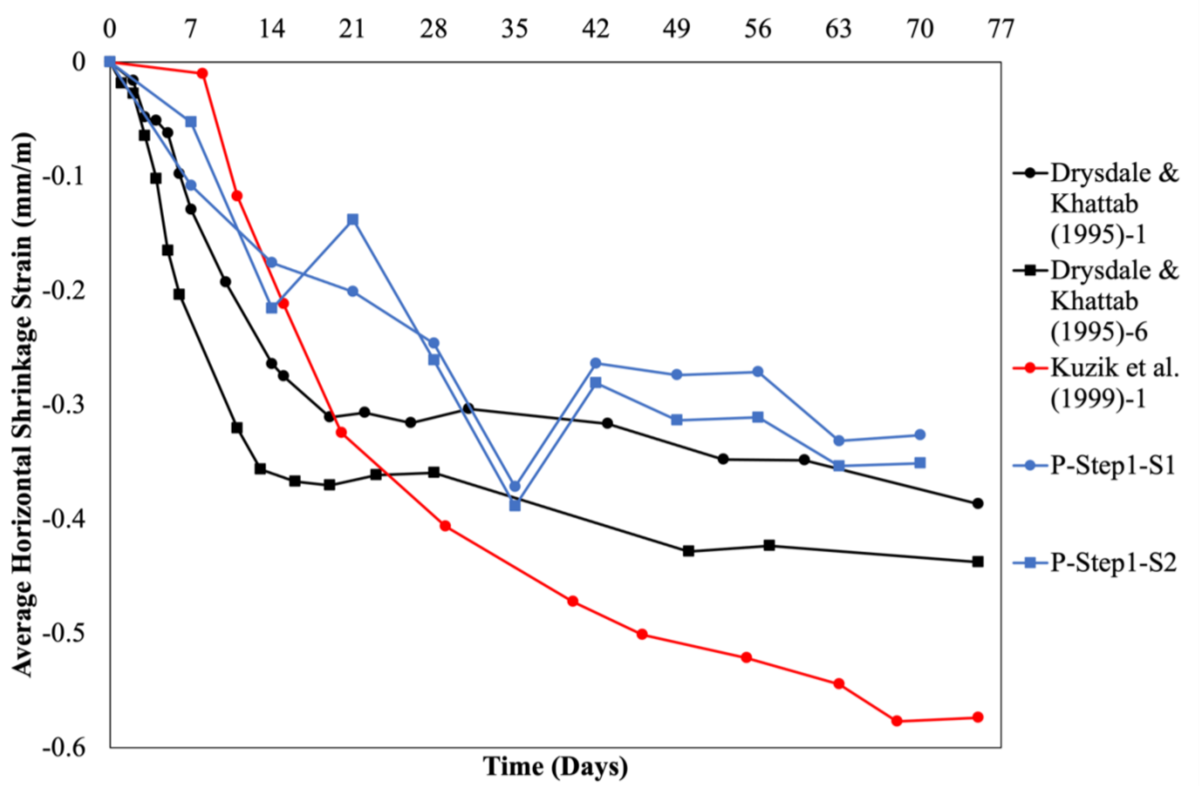

Figure 22: Average horizontal shrinkage for units in comparison to past studies from Drysdale & Khattab (1995) and Kuzik et al. (1999)

Moreover, vertical shrinkage results followed a similar trend to horizontal shrinkage as seen in Figure 23. On day 70, it was observed that the doublets exhibited horizontal shrinkage strains of -0.42 and -0.58 mm/m, while their vertical shrinkage strains were -0.53 and -0.54. Similarly, the triplets displayed horizontal shrinkage strains of -0.34 and -0.44 mm/m and vertical shrinkage strains of -0.54 and -0.57 mm/m. These results indicate that the influence of mortar joints on the shrinkage of concrete masonry assemblies is limited. This finding is supported by the fact that the vertical and horizontal shrinkage strains of both doublets and triplets have very close values.

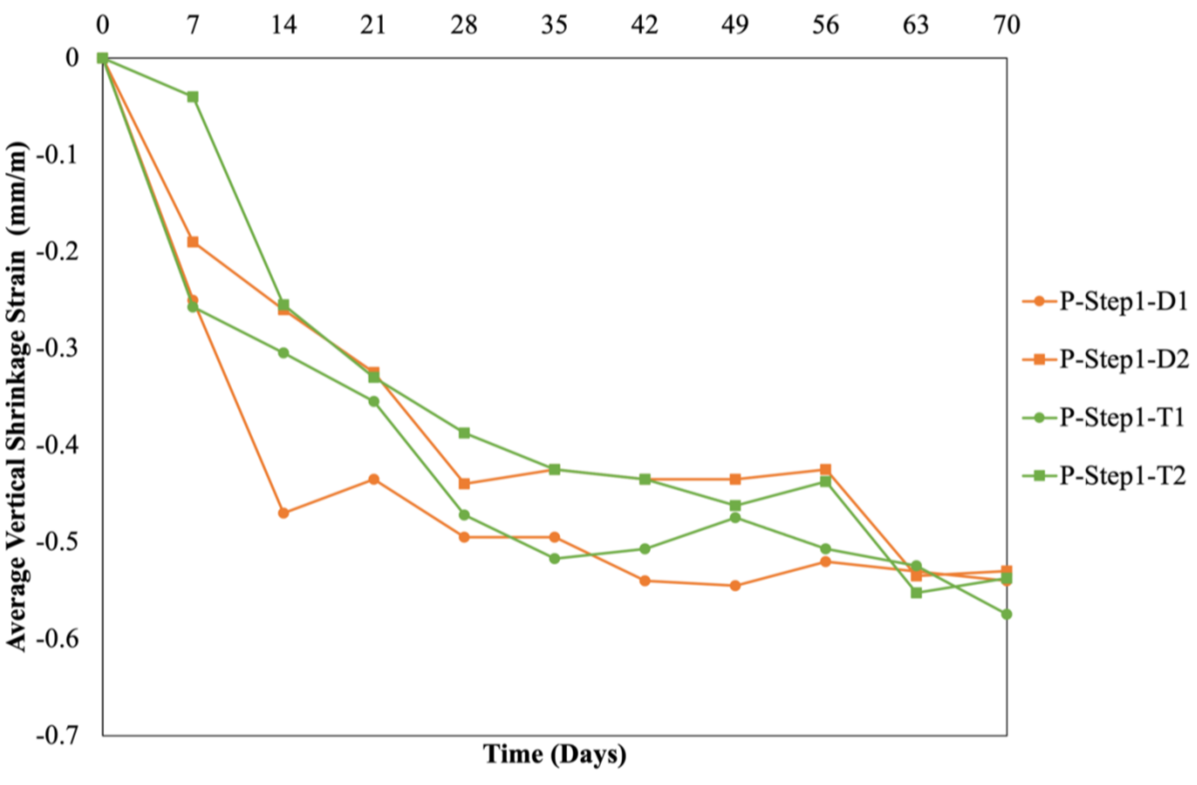

Figure 23: Average vertical shrinkage for each specimen versus time – across the mortar joint of faces

3.2 Preliminary results of drying shrinkage environmental testing – Step 2

In order to streamline the testing process and obtain preliminary results for step 2, single blocks were tested for oven-drying deformation measurements. The single blocks were removed from the controlled temperature oven and placed in a cooling chamber, where they were allowed to reach room temperature before taking the measurements. These blocks were not subjected to step 1 of the testing process, and the results were collected after 5 days, with subsequent measurements taken every other day until day 17. At this point, negligible weight changes were observed, as per ASTM C426-06 guidelines. Figure 24 depicts the shrinkage results obtained for two single blocks, which were compared to reference curves from ASTM C426-06. The analysis indicated that the experimental shrinkage strain curves of the single blocks exhibited a pattern similar to the ASTM standard, demonstrating comparable shrinkage patterns for both blocks. The plot of the reference curves and the experimental shrinkage strain curves indicated that the ultimate horizontal shrinkage was reached on day 17, with the values being remarkably similar. The ultimate horizontal shrinkage strain of the single blocks was found to be -0.32 and -0.38 mm/m, while the ASTM C426-06 standard yielded a value of -0.39 mm/m. These results highlight the consistency of the experimental data with the reference standard, which indicates the reliability of the testing methodology.

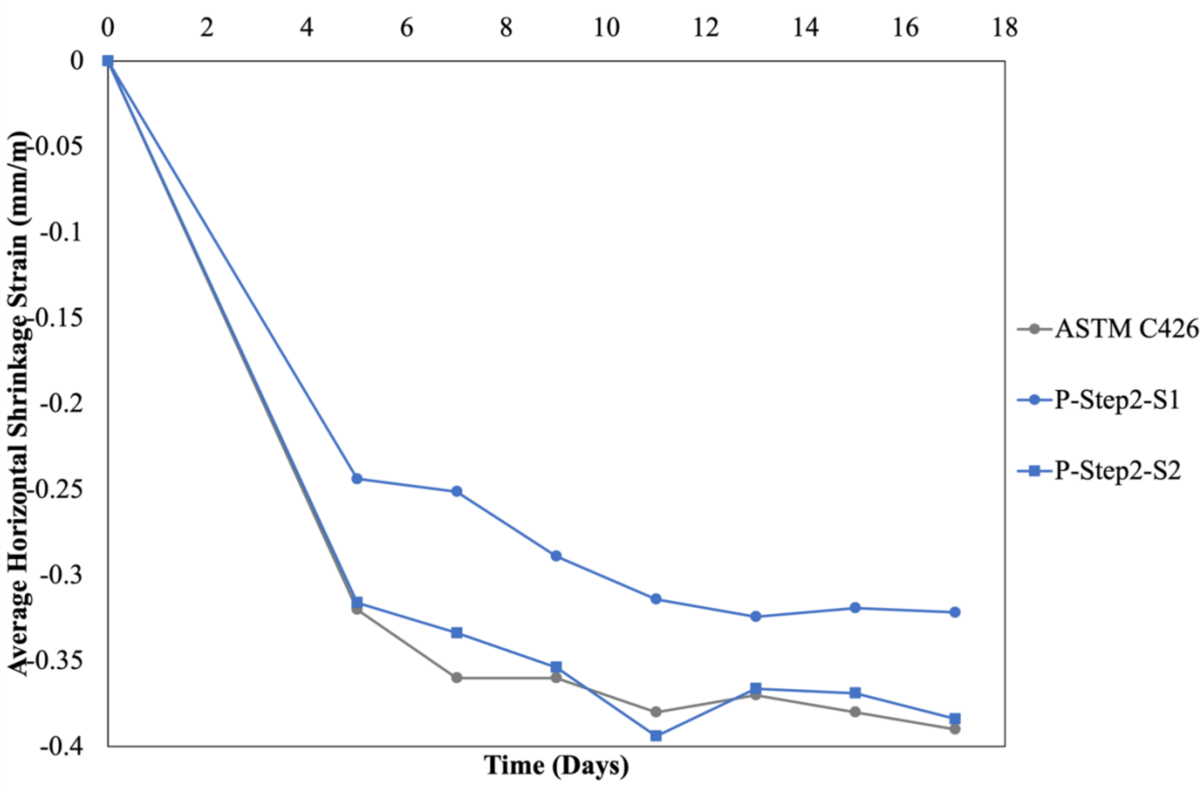

Figure 24: Average horizontal shrinkage for single units in comparison to ASTM C426

To obtain valuable insights into the 2-step procedure of this experiment, a comparison between the slow (step 1) and rapid (step 2) testing methods is illustrated in Figure 25. The ultimate shrinkage values reached at day 70 for step 1 were very similar to the ultimate shrinkage values obtained on day 17 for step 2. This finding suggests that the rapid testing method could provide comparable results to the slow testing method, potentially allowing for an efficient testing process. The ultimate horizontal shrinkage strain of the single blocks was found to be -0.32 and -0.38 mm/m for step 2 whereas it was -0.33 and -0.35 mm/m for step 1. It is worth noting that the peak registered around day 35 in step 1 may be due to measurement errors, and this is currently being investigated for future tests. Based on the observed trend for step 1, a better match with step 2 is expected to be obtained after day 84, which is the selected duration for the two-step testing.

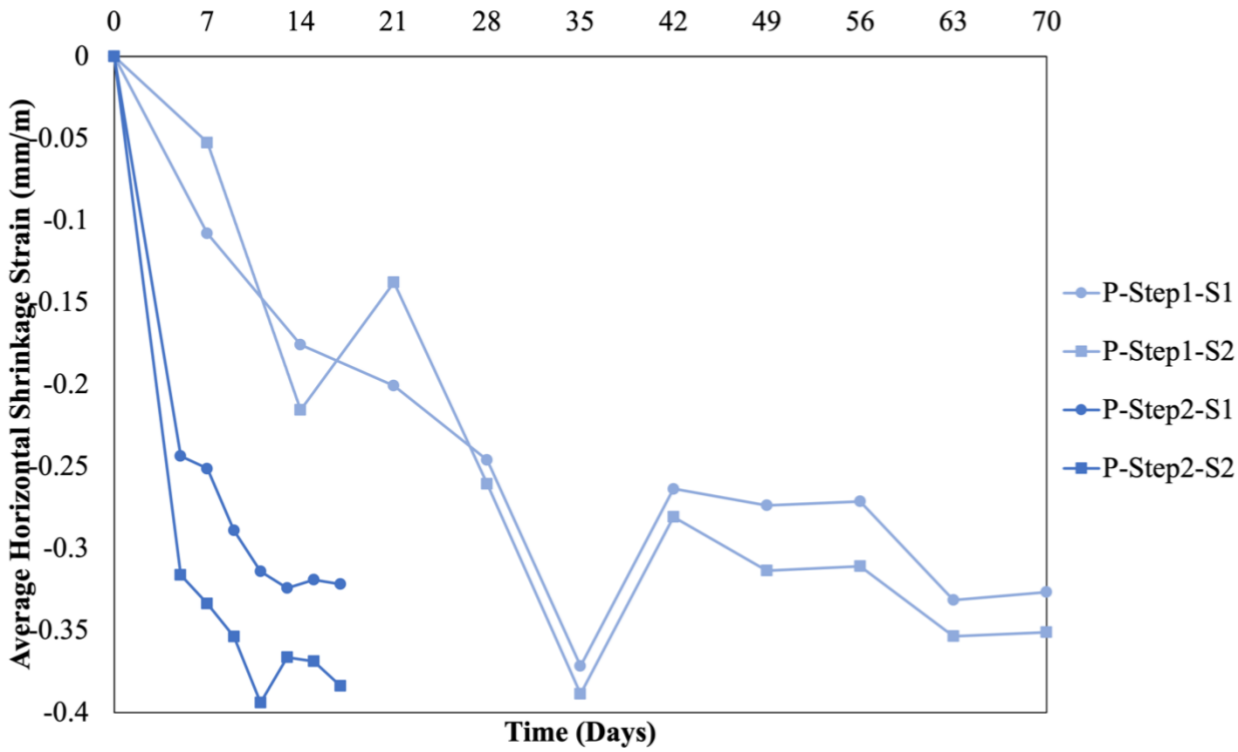

Figure 25: Average horizontal shrinkage for step 1 single units in comparison to step 2 single units

To further validate the findings from this experiment, data for step 2 on masonry prisms (doublets and triplets) and blocks previously tested in step 1 are also being collected. This will allow for a more comprehensive analysis of the shrinkage behaviour of concrete masonry structures and provide a more complete understanding of the factors that contribute to shrinkage.

3.3 New results of drying shrinkage environmental testing – Step 1

After the establishment of successful preliminary results, the experimental research progressed to gather new testing results. The data collection process is still ongoing, with the collection of data expected to continue for another year. The results of the thesis report on the findings collected thus far indicate progress. The new data set was collected using the same methodology as the preliminary data collection process, as discussed in the step 1 procedure. However, in order to increase accuracy, daily shrinkage strain measurements were taken for the first three weeks of the experiment, with weekly measurements taken for the remaining nine weeks. This was done to capture the maximum rate of shrinkage strain drop, which occurs during the initial weeks before stabilizing. To analyze the data further, the average of each horizontal and vertical measurement was calculated, with standard deviation values used to ensure accuracy. However, to reduce the volume of data, only selected data points were used to generate the curve in the following graphs, and outliers were removed. To remove outliers from the data, a visual analysis approach was employed. A cloud of data points was created, and each point was examined manually to identify any results that appeared to be significantly deviating from the observed shrinkage trend. Since measurements were taken daily generating more data for the analysis, it was possible to exercise an engineering judgment to determine whether a data point was an outlier based on its noticeable deviation from the overall pattern.

During this new phase of collecting results, daily air-drying shrinkage measurements were taken for 2 single concrete blocks, 2 doublets, and 2 triplets using a calibrated strain gauge over a period of 19 days. The results of these measurements were used to establish the initial patterns of shrinkage for each specimen. Figure 26 presents the horizontal shrinkage results across the long dimension of the faces of the new data collection and compares it to the preliminary results.

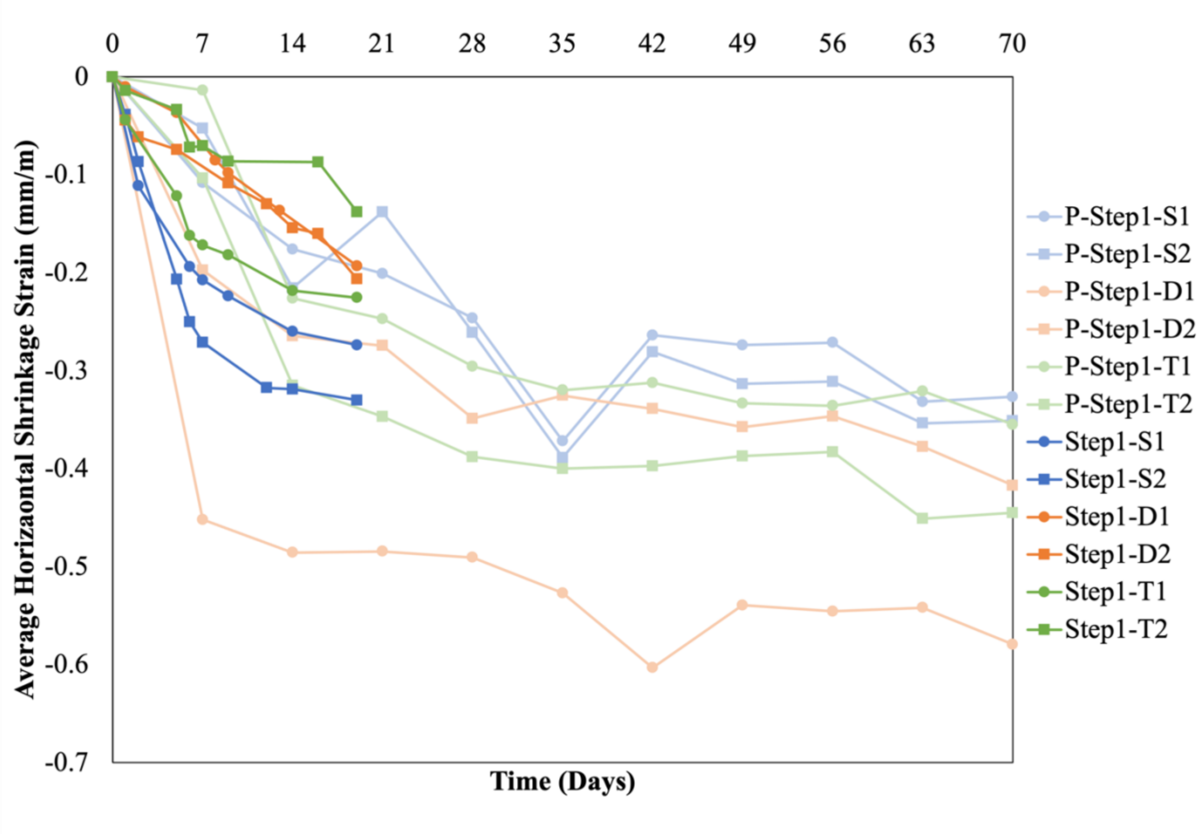

Figure 26: Average horizontal shrinkage for each specimen – new results in comparison to preliminary results

It is interesting to note that the new shrinkage strain follows an extremely similar pattern to the preliminary shrinkage strain, with the daily measurements successfully capturing the strong increase in shrinkage during the initial days of the experiment. However, unlike what was seen in the preliminary results, the new results also revealed that the units were shrinking faster than the masonry specimens. This change could be attributed to the different block palettes used in the preliminary and new experiments. To confirm this assumption, further testing will be required, and additional data collection will need to be conducted to determine the source of these slight discrepancies. Nonetheless, the current findings demonstrate that the methodology used in this study has the potential to yield accurate and reliable drying shrinkage results. These new results also confirm the speculation made earlier that Step1-D1 results have some measurement error. This could be to misplaced strain gauges and a human error in the initial measurement.

To ensure the accuracy and validity of the results obtained, a comparison was made between the new shrinkage results of the two single concrete blocks used in this study and the results of previous studies conducted by Drysdale and Khattab (1995) and Kuzik et al. (1999). Figure 27 illustrates the comparison between these new results and the preliminary results.

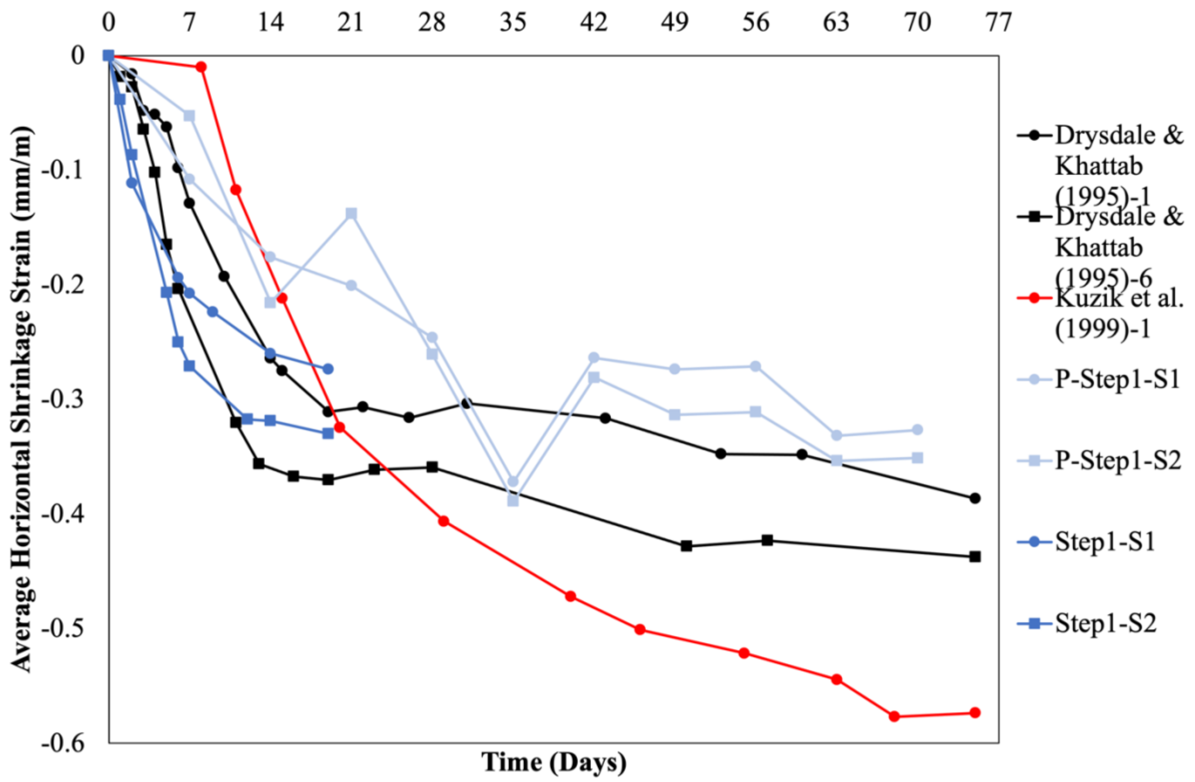

Figure 27: Average horizontal shrinkage for units in comparison to past studies – new results in comparison to preliminary results

All the shrinkage plots for each block appear to follow a similar overall trend. It is worth noting that the disparities observed in the comparison between the results of this study and previous research were further reduced due to the increased accuracy achieved with the daily shrinkage measurements in the new data collection, as compared to the weekly measurements used in the preliminary phase. Interestingly, the average shrinkage identified in the new results is no longer lower than that reported in the previous research, which is a significant finding. The new results match even better with the Drysdale and Khattab (1995) results. This finding is a positive indication that the rest of the data that will be collected in the ongoing tests will likely result in a curve that yields very similar to the curves reported in the previous studies.

In addition to the horizontal shrinkage results, the vertical shrinkage results obtained in both the preliminary and new phases of the experiment also showed a similar trend, as depicted in Figure 28.

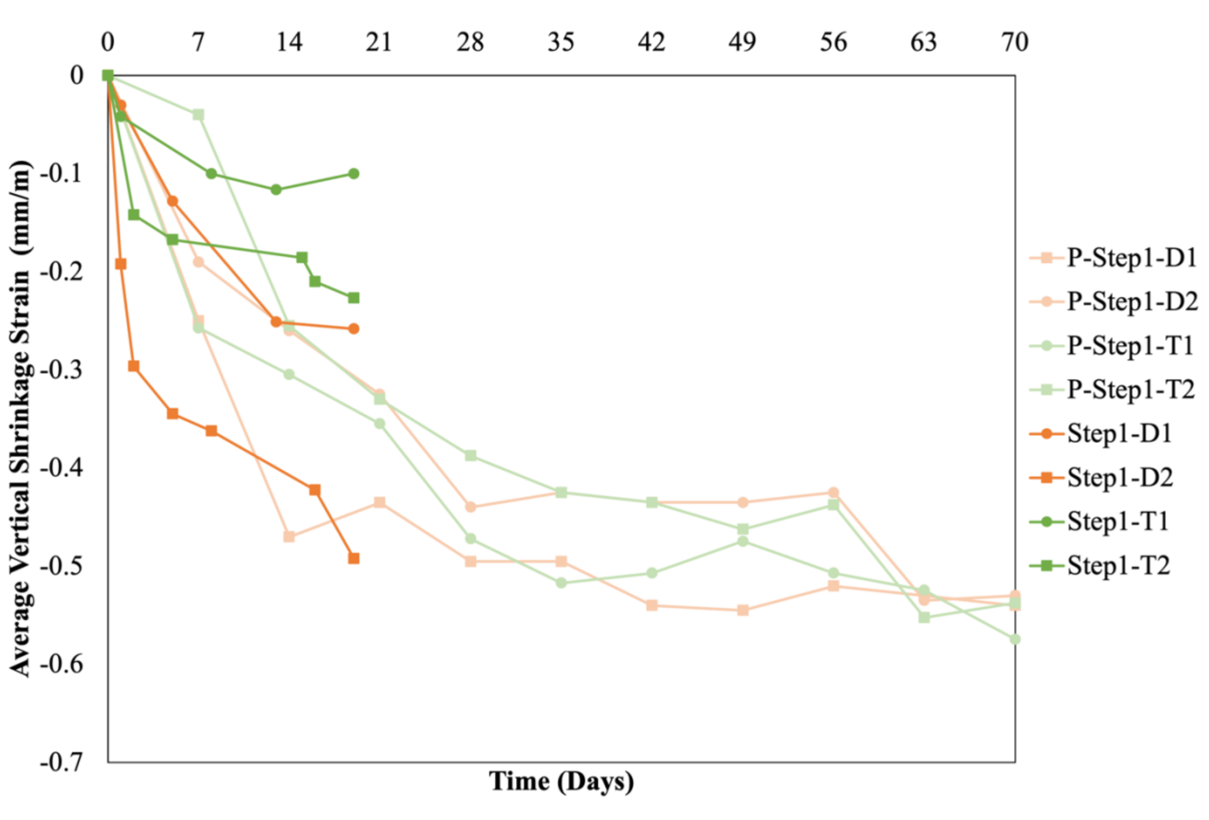

Figure 28: Average vertical shrinkage for each specimen – new results in comparison to preliminary results

This finding suggests once again consistency in the results obtained in both the horizontal and vertical shrinkage measurements. The influence of mortar joints on the shrinkage of concrete masonry assemblies is therefore proven to be limited. It is important to note that these new results are still only for the first 19 days of the experiment out of the total 84 days. As a result, some discrepancies are observed in the curves, especially when comparing them with the preliminary results.

Furthermore, it is worth noting that the horizontal shrinkage strain measurements are taken over the uniform face of a block, while the vertical shrinkage strain is taken across the mortar joint. Consequently, the vertical measurements exhibited slightly more variations due to the combined effect of the shrinkage of the mortar and a portion of the block, a non-uniform surface. However, with more data on the way, it is anticipated that the curves for vertical drying shrinkage will exhibit a more apparent trend, allowing for a more thorough analysis of the data.

3.4 New results of drying shrinkage environmental testing – Step 2

In order to measure oven-drying deformation, 5 single blocks were tested in step 2 of the experiment, without going through step 1. The results were collected over a period of 17 days, with measurements taken after 5 days and then every other day, following the initial surface-saturated dry measurement. As per the guidelines of ASTM C426-06, negligible weight changes were observed when day 17 was reached, indicating that ultimate shrinkage had been achieved for the single blocks. Figure 29 depicts the shrinkage results obtained from the 5 single blocks, which were compared to the preliminary shrinkage results and the reference curve from ASTM C426-06.

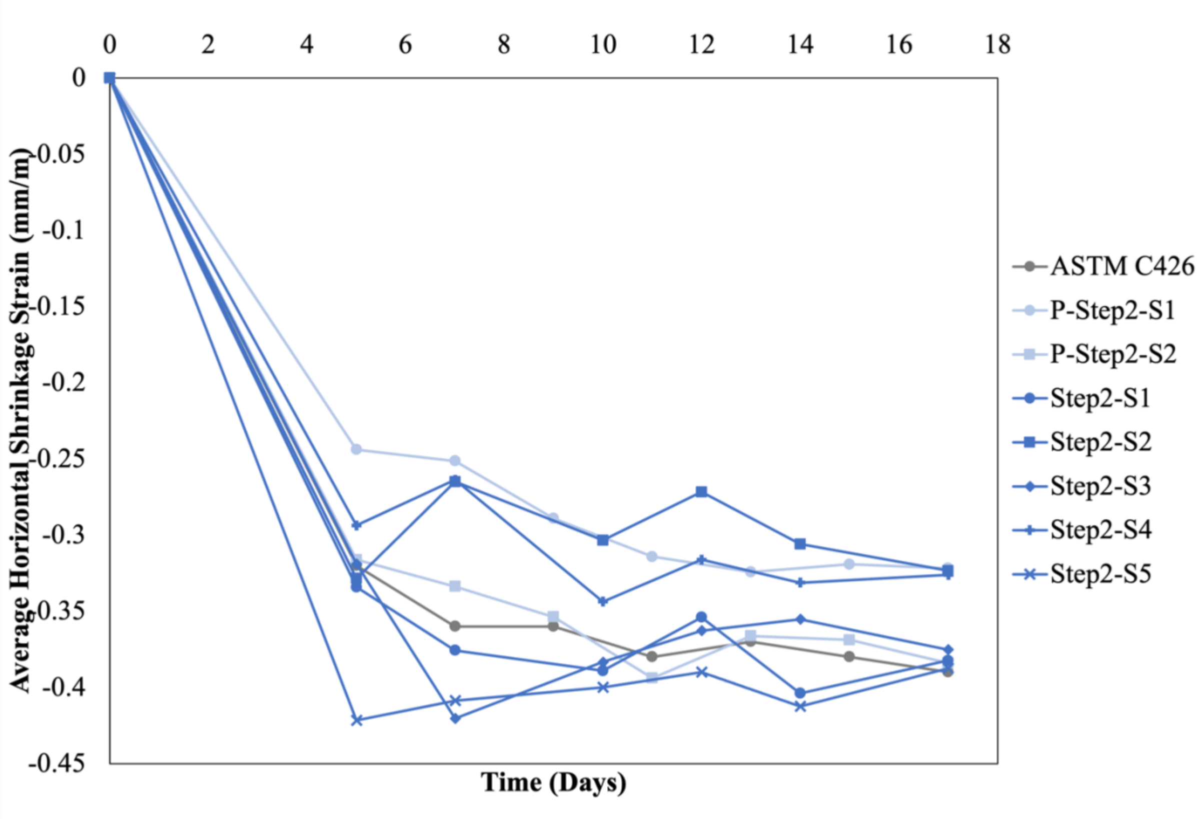

Figure 29: Average horizontal shrinkage for single units – new results in comparison to preliminary results and ASTM C426

All curves demonstrated similar shrinkage patterns, indicating that ultimate horizontal shrinkage was reached on day 17 with similar values. Despite slight variations in the measurements, which may have been due to human error when holding the strain gauge, the trend observed proves that the collected results are in accordance with the ASTM C426-06 standard. Thus, the rapid process of shrinkage using an oven in step 2 accurately measures ultimate shrinkage.

The preliminary and ongoing new results have provided a reliable point of reference to validate the accuracy of the newly developed 2-step drying shrinkage procedure. The shrinkage data and plot that were presented above have successfully demonstrated that the results are comparable to previous studies and standards. With the experiment still in progress, more results will be collected over the following year. These will include more single blocks, doublets, triplets, mortar prisms, and 5 masonry stacked prisms, all of which will undergo step 1 for 84 days, followed by step 2. With this additional data, it will be possible to identify more possible reasons for the slight discrepancies that may occur, although they are mostly negligible. These results will also serve as an excellent database for future research, as it represents the first time that masonry specimens have been tested for drying shrinkage.

4 CONCLUSIONS

The issue of climate change has been a topic of concern in recent years, and standards related to cavity-wall design have been identified as priorities for climate change adaptation provisions. The Canadian Standards Association (CSA) Group has released technical reports highlighting the importance of adapting masonry design to climate change. To address this need, as part of a larger research program led by the McGill struct-lab and sponsored by various industry and institutional partners, this study investigates the linear drying shrinkage response of concrete masonry blocks, assemblies, and mortar samples. The research fills current knowledge gaps through the characterization of the environmental performance of cavity-wall components through laboratory tests. This will involve the calibration of new design approaches based on experimental outcomes and the evaluation of climate-adapted design options for archetypical building sub-systems under different loading conditions. This will help identify potential criticalities related to larger cavity widths and shelf angles, as well as the layout of movement joints. The purpose of this thesis paper is to inform the national research community of the main objectives of this transformative project, as well as to discuss preliminary and ongoing new results related to the structural characterization of concrete masonry blocks and assemblies. A new 2-step drying shrinkage procedure is proposed to enable obtaining both strains versus time curves needed for numerical modelling and the ultimate values required for practical design in a reasonable timeframe.

Preliminary results indicate that the linear drying shrinkage behaviour of modern concrete masonry blocks appears to be in good agreement with that inferred experimentally by previous Canadian researchers in 1995 and 1999. The study also reveals that mortar joints have a limited effect on the shrinkage behaviour of masonry assemblies. Doublets and triplets without vertical joints exhibited similar shrinkage performance when compared to individual blocks, even when normalized results were compared. Moreover, the study compared the results for step 2 (accelerated drying shrinkage test) for individual concrete blocks not previously subjected to step 1 (slow drying shrinkage test) to those inferred from step 1 alone. The comparison revealed that for the specimens tested, the selected duration of 84 days for the ultimate values is reasonable, as they were similar. These preliminary results have enabled us to confirm that the proposed new testing methodology is reliable and accurate. With the positive preliminary results, the research has been able to move to its next phase of collecting final results. The current ongoing final results have shown promising agreement with previous Canadian research. As the research continues, updated and more comprehensive results will be shared with the research and professional communities.

Despite the limitations, the findings of this study provide valuable insights into the behaviour of masonry structures under climate change risks. The results suggest that the slow testing method (step 1) combined with the rapid testing method (step 2) used in this research can be used to assess the drying shrinkage of masonry structures accurately. The methodology can also be used to identify the most appropriate adaptation strategies for the climate-resilient design of concrete masonry infrastructures.

Further research is needed to explore the impact of different climate change risks on the behaviour of masonry structures. The findings of this research can be used as a foundation for future research in this area. Overall, the research underscores the importance of climate-resilient design adaptation of concrete masonry infrastructures and the need for innovative solutions to address the challenges posed by climate change.

5 REFERENCES

Aarle, M. V., Schellen, H., & Schijndel, J. V. (2015). Hygro Thermal Simulation to Predict the Risk of Frost Damage in Masonry; Effects of Climate Change. *6th International Building Physics Conference* (pp. 2536 – 2541). Torino, Italy: Energy Procedia.

American Society for Testing and Materials. (2006). *ASTM C426-06 Test Method for Linear Drying Shrinkage of Concrete Masonry Units.* ASTM International.

American Society for Testing and Materials. (2007). *ASTM C490-07 Standard Practice for Use of Apparatus for the Determination of Length Change of Hardened Cement Paste, Mortar, and Concrete.* ASTM International.

American Society for Testing and Materials. (2009). *ASTM C462-09 Standard Test Method for Linear Drying Shrinkage of Concrete Masonry Units.* ASTM International.

American Society for Testing and Materials. (2018). *ASTM C596-18 Standard Test Method for Drying Shrinkage of Mortar Containing Hydraulic Cement.* ASTM International.

American Society for Testing and Materials. (2019). *ASTM C270-19 Standard Specification for Mortar for Unit Masonry.* ASTM International.

American Society for Testing and Materials. (2020). *ASTM C1437-20 Standard Test Method for Flow of Hydraulic Cement Mortar.* ASTM International.

Baker, C., Marr, J. K., & Drysdale, R. G. (2004). Capacity of Single and Double Wythe Unfeinforced Concrete Block Walls. *13th International Brick and Block Masonry Conference*.

Booya, E., Ghaednia, H., Das, S., & Pande, H. (2018). Durability of cementitious materials reinforced with various Kraft pulp fibers. *Construction and Building Materials*, 1191–1200.

Brick Industry Association. (2006). *Volume Changes – Analysis and Effects of Movement.* Reston, Virginia: Brick Industry Association.

Bush, E., & Lemmen, D. S. (2019). *Canada's Changing Climate Report.* Environment and Climate Change Canada.

Canada Infrastructure Bank. (2020). *$10B Investment Plan to Grow the Economy and Create Jobs.* Ottawa: Canada Infrastructure Bank.

Canadian Standards Association. (2004). CSA A165.1 Concrete Block Masonry Units. *CSA A165 Series*.

Canadian Standards Association. (2004). CSA S304.1 Design of Masonry Structures. *CSA.*

Canadian Standards Association. (2014). CSA A165.1-14 Concrete Block Masonry Units. *CSA.*

Canadian Standards Association. (2014). CSA A370-14 Connectors for Masonry. *CSA.*

Canadian Standards Association. (2014). CSA S304-14 Design of Masonry Structures. *CSA.*

Cannon, A. J., Jeong, D., Zhang, X., & Zwiers, F. W. (2020). *Climate-resilient buildings and core public infrastructure 2020 : an assessment of the impact of climate change on climatic design data in Canada.* Gatineau: Environment and Climate Change Canada.

Cavalagli, N., Kita, A., Castaldo, V. L., Pisello, A. L., & Ubertini, F. (2019). Hierarchical environmental risk mapping of material degradation in historic masonry buildings: An integrated approach considering climate change and structural damage. *Construction and Building Materials, 215,* 998-1014.

Corradi, M., Tedeschi, C., Binda, L. A., & Borri, A. (2008). Experimental Evaluation of Shear and Compression Strength of Masonry Wall Before and After Reinforcement: Deep Repointing. *Construction and Building Materials, 4,* 22.

Dias, J. M. (2002). Movement in Masonry Walls Caused by Temperature and Moisture Changes. *Sixth International Masonry Conference.*

Drysdale , R. G., & Khattab, M. (1995). Shrinkage Characteristics of Concrete Blocks. *7th Canadian Masonry Symposium*.

Environment and Climate Change Canada. (2016). *Pan-Canadian Framework on Clean Growth and Climate Change : Canada's plan to address climate change and grow the economy.* Gatineau: Environment and Climate Change Canada.

Environment and Climate Change Canada. (2022). *Preparing for Climate Change Canada's National Adaptation Strategy.* Gatineau: Environment and Climate Change.

Gaur, A., Lacasse, M., & Armstrong, M. (2019). Climate Data to Undertake Hygrothermal and Whole Building Simulations Under Projected Climate Change Influences for 11 Canadian Cities. *Data, 4*(2), 72.

Gorospe, K., Dhaednia, H., & Das, S. (2019). Effect of various glass aggregates on the shrinkage and expansion of cement mortar. *Construction and Building Materials*, 301–311.

Government of Canada. (2022, 02 21). *Developing climate resilient standards and codes*. Retrieved from Canada.ca: https://www.canada.ca/en/environment-climate-change/services/climate-change/canadian-centre-climate-services/basics/developing-climate-resilient-standards-codes.html#toc3

Goyal, A., Hatzinikolas, M. A., & Warwaruk, J. (1992). *Differential Movement in Cavity Walls and Veneer Walls Due to Material and Environmental Effects.* Canadian Masonry Research Institute.

Hall, C., Hamilton, A., Hoff, W. D., Viles, H. A., & Eklund, J. A. (2010). Moisture dynamics in walls: response to micro-environment and climate change. *The Royal Society, 467*(2125).

Hatzinikolas, M., Longworth, J., & Warwaruk, J. (1982). *Strength and Behaviour of Metal Ties in 2-wythe Masonry Walls.* Alberta Masonry Institute - FERO Corp Technical Report.

Idiart, A. E. (2009). *Coupled Analysis of Degradation Processes in Concrete Speciments at the Meso-level.* Barcelona, Spain.

Ismaiel, M., Chen, Y., Cruz-Noguez, C., & Hagel, M. (2021). Thermal Resistance of Masonry Walls: A Literature Review on Influence Factors, Evaluation, and Improvement. *Journal of Building Physics*, 1-40.

Jianxia, S. (2012). 6.14 Durability Design of Concrete Hydropower Structures. In S. Jianxia, *Comprehensive Renewable Energy* (pp. 377-403). Yangzhou: Elsevier.

Kubba, S. (2017). Chapter Nine - Impact of Energy and Atmosphere. In S. Kubba, *Handbook of Green Building Design and Construction* (pp. 443-571). Oxford: Joe Hayton.

Kuzik, M. D., Elwi, A. E., & Hatzinikolas, M. A. (1999). Long-term Differential Movement in Masonry Cavity Walls. *8h North American Masonry Conference.* Austin, Texas.

Lacasse, M. A., Gaur, A., & Moore, T. V. (2020). Durability and Climate Change-Implications for Service Life Prediction and the Maintainability of Buildings. *Buildings, 10*(3), 53.

Lacasse, M. A., Ge, H., Hegel, M., Jutras, R., Laouadi, A., Sturgeon, G., & Wells, J. (2018). Guideline on Design for Durability of Building Envelopes. *National Research Council of Canada*, 35.

Lohonyai, A. J., Korany, Y., & Gül, M. (2015). Remote Field Monitoring of Thermal and Moisture Deformations in Masonry Cavity Wall Building Envelopes. *Journal of Performance of Constructed Facilities*, *29*(3), 04014072.

Mekis, É., & Vincent, L. A. (2011). An Overview of the Second Generation Adjusted Daily Precipitation Dataset for Trend Analysis in Canada. *Atmosphere-Ocean*, *49*(2), 163-177.

Menun, A., Das, T., Saad, L., Sparling, A., & Malomo, D. (2023). A new 2-step testing method for measuring moisture-induced shrinkage of concrete blocks, mortar and masonry assemblies . *14th North American Masonry Conference.* Omaha: 14NAMC.

Morice, C. P., Kennedy, J. J., Rayner, N. A., & Jones, P. D. (2012). Quantifying uncertainties in global and regional temperature change using an ensemble of observational estimates: The HadCRUT4 data set. *Journal of Geophysical Research Atmospheres*.

National Round Table on the Environment and the Economy. (2011). *2010-11 Departmental Performance Report.* Ottawa: NRTEE.

National Round Table on the Environment and the Economy. (2011). *Paying the Price: The Economic Impacts of Climate Change for Canada.* Library and Archives Canada.

Pravin, S. N., Murali, K., & Shanmugapriyan, R. (2017). Review on Climate Change and its Effects on Construction Industry. *International Research Journal of Engineering and Technology, 04*(11), 1180-1183.

Ritchie, T. (1961). Cavity walls. *National Research Council of Canada Publications Archive*.

Saha, M., & Eckelman, M. J. (2014). Urban scale mapping of concrete degradation from projected climate change. *Urban Climate, 9*, 101-114.

Saxer, E. L., & Toennies, H. T. (1957). Measuring Shrinkage of Concrete Block – A Comparison of Test Methods. 988-1004.

Shrive, N. G., Sayed-Ahmed, E. Y., & Tilleman, D. (1997). Creep Analysis of Clay Masonry Assemblages. *Canadian Journal of Civil Engineering, 24*(3), 367–379.

Sparling, A., Palermo, D., & Khan, U. T. (2021). *Climate Change Adaptation of Masonry Materials, Design, and Construction.* Canadian Standards Association.

Straka, V. A. (2005). Environmental Impact of Masonry Industry. *10th Canadian Masonry Symposium*.

Sturgeon, G. (2012). Physical Properties. *Metric Technical Manual*.

Talukdar, S., & Banthia, N. (2013). Carbonation in concrete infrastructure in the context of global climate change: Development of a service lifespan model. *Construction and Building Materials, 40*, 775-782.

The American Instituite of Architects. (2017). Chapter 6: Masonry. In T. A. Architects, *Architectural Graphic Standards Student Edition* (pp. 6-35). Hoboken: Wiley.

The Council of Canadian Academies. (2019). *Canada's Top Climate Change Risks.*

Vandemeulebroucke, I., Defo, M., Lacasse, M. A., Caluwaerts, S., & Van Den Bossche, N. (2011). Canadian Initial-Condition Climate Ensemble: Hygrothermal Simulation on Wood-Stud and Retrofitted Historical Masonry. *Building and Environment, 187*, 107318.

Vincent, L. A., Zhang, X., Brown, R. D., Feng, Y., Mekis, É., Milewska, E. J., & Wang, X. L. (2015). Observed trends in Canada's climate and influence of low-frequency variability modes. *Journal of Climate*, 4545–4560.

Warren, F. J., Barrow, E., Schwartz, R., Andrey, J., Mills, B., & Riedel, D. (2004). *Climate Change Impacts and Adaptation: A Canadian Perspective.* Ottawa: Natural Resources Canada.

Wittmann, F. H. (1993). On the Influence of Stress on Shrinkage of Concrete. *Creep and Shrinkage of Concrete*, 151-157.

Yoon, I.-S., Çopuroğlu, O., & Park, K.-B. (2007). Effect of Global Climatic Change on Carbonation Progress of Concrete. *Atmospheric Environment, 41*(34), 7274-7285.

Zhou, X., Carmeliet, J., & Derome, D. (2020). Assessment of Risk of Freeze-thaw Damage in Internally Insulated Masonry in a Changing Climate. *Building and Environment, 175*, 106773.